Monitoring the Transport of Microorganisms in Aquatic Environments Using Unmanned Surface Vehicles

Craig W. Powers

Dissertation submitted to the faculty of the
Virginia Polytechnic Institute and State University
in partial fulfillment of the requirements for the degree of

Doctor of Philosophy
in
Civil Engineering

Linsey C. Marr, Co-Chair
David G. Schmale III, Co-Chair
Shane D. Ross
John C. Little

December 18, 2017
Blacksburg, Virginia

Keywords: bioaerosol, plume, air water interface, unmanned surface vehicle, hazardous agent

Monitoring the Transport of Microorganisms in Aquatic Environments Using Unmanned Surface Vehicles

Craig W. Powers

(Academic Abstract)

The majority of the Earths surface is covered with water, and the air-water interface (AWI) acts as the natural boundary between the atmosphere and the water. The AWI is an important ecological zone in natural aquatic habitats that governs transport of material and energy between bodies of water and the atmosphere. Little is known about temperature profiles and biological transport across the boundary layers at the air-water interface, and how wind interactions at the AWI affects them. New technologies such as sensors and unmanned surface vehicles (USV) need to be developed and used to address this knowledge gap. The goal of the research is to study population densities of the bacteria *Pseudomonas syringae* below, at and above the AWI using USV equipped with specialized sensors.

The first specific objective was to map temperature profiles and resolve the boundary layer at the AWI using high resolution distributed temperature sensing (HR-DTS) on board an unmanned surface vehicle (USV).

Our second research objective was to sample microbes from the water with a USV at multiple depths and locations.

Our third research objective was to sample microbes from the atmosphere with a USV at the AWI.

Our fourth research objective was to track and localize hazardous agents (tracer dyes) using a USV in aqueous environments.

Monitoring the Transport of Microorganisms in Aquatic Environments Using Unmanned Surface Vehicles

Craig W. Powers

(General Audience Abstract)

The majority of the Earths surface is covered with water, and the air-water interface (AWI) acts as the natural boundary between the atmosphere and the water. The AWI is an important ecological zone in natural aquatic habitats. Little is known about temperature profiles and biological transport across the boundary layers at the air-water interface, and new technologies need to be developed and used to address this knowledge gap. The specific objectives of the proposed work are to: (1) map temperature profiles and resolve the boundary layer at the AWI using high resolution distributed temperature sensing (HR-DTS) on board an unmanned surface vehicle (USV), (2) sample microbes from the water with a USV at multiple depths and locations, (3) sample microbes from the atmosphere with a USV at the AWI, and (4) track and localize hazardous agents (tracer dyes) using a USV in aqueous environments.

Acknowledgments

The work presented here would not be possible without the opportunities made possible by my co-advisors, Dr. Linsey Marr and Dr. David Schmale. It is with profound gratitude that I acknowledge their continued patients and guidance, that without, I assuredly would not have been successful. I would like to thank my committee, Dr. Little and Dr. Ross for their wise words, advice and encouragement. Thank you for helping me to stay the course.

It has been a great pleasure to be a part of the Schmale Lab and Applied Interdisciplinary Research in Air (AIR^2) groups. I would like to thank all the group members for sharing their time and passion for research. In particular, I would like to say thank you to all the Schmale lab members that have contributed directly to my research success including Mr. Christopher Anderson; Mr. Jamie Benson; Ms. Hope Gruszewski; Ms. Regina Hanlon; Ms. Niki McMaster; Ms. Celia Sanchez; and Ms. Nina Wilson.

I would like to thank Ms. Terri Bourdon, Dr. Chung, Dr. Rogers, Dr. Rossi, and Ms. Jessica Schmale for their kindness and guidance during my attendance during my time at the Mathematics Department .

Finally, I would like to thank my fiancée, Kasia Świrydowicz, for her patience, love and support, and for all the adventures we have had and will have together.

This work was supported in part by seed grants to Dr. Schmale from the Institute of Critical Technology and Applied Science (ICTAS) (Environmental Sensing of the Atmosphere and Water with Fiber Optic Lines) and the College of Agriculture and Life Sciences at Virginia Tech, the National Science Foundation (NSF) (Research on Airborne Ice-Nucleating Species (RAINS)), (Integrative Graduate Education and Research Traineeship: MultiScale Transport in Environmental and Physiological Systems (MultiSTEPS)), and (NRI: Coordinated Detection and Tracking of Hazardous Agents with Aerial and Aquatic Robots to Inform Emergency Responders), (HAZARDS SEES: Uncovering the Hidden Skeleton of Environmental Flows: Advanced Lagrangian Methods for Hazard Prediction, Mitigation, and Response)

Contents

List of Figures

List of Tables

Chapter 1. Introduction

1.1 Background and Motivation

The air water interface (AWI) is possibly the most common liquid interface and impacts atmospheric, aerosol and environmental chemistry (Stiopkin et al., 2011). Specifically, the marine atmospheric boundary layer (MABL), the boundary where the atmosphere touches the global ocean surface (Garratt, 1994), represents the largest boundary of our planet's surface area making this boundary of great importance to global dynamics. Many environmental processes are influenced by this boundary, and transport across this interface is limited by viscous boundary layers on both sides of the AWI (Garbe et al., 2014). Turbulence, which occurs often in aquatic environments due to water motion, wind interaction and tides, can change the rate of transport across the AWI (Kinsman, 1965). Many AWI transport models have been proposed but real world data is needed to validate these models and to gain an improved understanding of these transport mechanisms (Law and Khoo, 2002). Most often, due to the properties of water and air, transport is dictated by dynamics of the water below the AWI (Xu et al., 2006). Compared to other substances, water has a high heat capacity and in the form of oceans, it has the highest capacity in the global climate system (Willis et al., 2004). Thermal energy energy from the sun that is not reflected by clouds or other particulate matter is absorbed and radiated at the AWI (Faizal and Rafiuddin Ahmed,

2011). Abiotic (non-living) and biotic (living) particles cross the AWI through deposition and aerosolization processes. Transport across the AWI impact global scale dynamics such as cloud formation, weather, spread of disease, ocean acidification and climate (Samset, 2016). understanding transport across the AWI is crucial to understanding the mechanisms behind these Earth processes.

Thermal energy from the sun that is not reflected by the atmosphere is transported to oceans and lakes through the AWI. At this boundary, this energy is reflected, or converted into sensible heat and different forms of energy where it is stored by oceans and lakes (Faizal and Rafiuddin Ahmed, 2011). This energy can be radiated and transported long distances, impacting the Earth's global energy budget and contributing to ocean phenomena such as currents, atmospheric weather and climate (Trenberth et al., 2009). This stored energy influences the temperature of oceans and can have a large impact on the concentration of gases that have be transported across the AWI (Garbe et al., 2014). Anthropogenic increases in atmospheric gases such as CO_2 and free elements such as sulfur and nitrogen (Schwede and Lear, 2014) are increasingly absorbed and held in solution by oceans decreasing pH and subsequently increasing acidification. This can have devastating impact on sea life throughout the oceans (Sabine et al., 2004). Using current modeling techniques, a drastic increase in acidity in the global ocean from past volcanic eruptions 252 million years ago, has recently been linked to one of our planet's largest mass extinctions underscoring the importance of this phenomena (Clarkson et al., 2015). Determining heat flux across the AWI is difficult for many reasons such as sea state condition, variable wind speeds and remote distances (Valdivieso et al., 2017). Satellite sea surface temperature measurements can and have been used, but can be prone to errors in sampling and cloud identification (Liu and Minnett, 2016; Viswambharan et al., 1986). Accurate in situ measurements at the AWI interface are important and needed to understand long term climate and weather effects.

The AWI serves as a physical boundary between microorganisms that live in aquatic environments and microorganisms that can aerosolize and survive transportation through the atmosphere e.g., the bacterium *Pseudomonas syringae*, (Morris et al., 2008). *Pseudomonas syringae* and other microorganisms are ubiquitous in the atmosphere and have been found in abundance in oceans and lakes (Bauer et al., 2002; Pietsch et al., 2017). Some microorganisms are pathogens of crops, domestic animals, and humans (Polymenakou, 2012). Bacteria in marine environments can reach the AWI where they may become aerosolized into the atmosphere from the sea-surface micro-layer (SML) inside small droplets by interactions with breaking waves at the coasts, and in whitecaps on wind driven waves in the open ocean (Wu, 1981; Li et al., 2017). The primary means of microbial aerosolization from aquatic surfaces is usually attributed to bubble bursting (Blanchard, 1989). If these aerosols have enough momentum and the proper trajectory they can escape into the atmosphere and be transported kilometers through the atmosphere (Schmale III and Ross, 2015; Mishchuk and Goncharuk, 2011). These aerosols can then travel back to terrestrial or aquatic environments through dry and wet deposition (Weerasundara et al., 2017). The concentrations and size distributions of airborne microorganisms around the globe are understudied (Burrows et al., 2009). Understanding the aquatic sources and abundance of these microorganisms that may become aerosols is important to understanding health and disease in humans crops and livestock that may be impacted by this transport.

Some bacteria, such as *P. syringae* and *Xanthomonas campestris*, may have a direct impact on the water cycle and global precipitation (Morris et al., 2008). Some strains of these bacteria are known to exhibit ice nucleation active (INA) proteins which can organize water molecules and allow water to freeze at much warmer temperatures than would be possible for pure water (Hill et al., 2014) . This enables these particular bacteria to serve as biogenic ice nuclei of water droplets and ice crystals initiating precipitation events such as rain and

snow (Blanchard, 1989; Christner et al., 2008b; Pöschl et al., 2010). Microbial ice nucleators are amongst the most efficient ice nucleation particulates in the atmosphere allowing for ice formation at temperatures as high as -2°C (Christner et al., 2008a). Ice nucleation is responsible for most of the precipitation over land and impacts the lifetime and structure of clouds (Polen et al., 2016). *P. syringae* is found in abundance in terrestrial and aquatic environments (Morris et al., 2008; Faizal and Rafiuddin Ahmed, 2011; Pietsch et al., 2017) and has been associated with nearly all components of the water cycle (Morris et al., 2013). Studying this transportation cycle of microorganisms such as *P. syringae* is a crucial part of understanding the current and future state of the global and local environments that rely on precipitation to allow plant and animal life to thrive.

New technology with unmanned vehicles (UVs) operating in the air, water and land, are increasingly being used in fields of study including climate, weather and water, ecosystem monitoring and management, and coastal mapping (Pereira et al., 2009). Use of primitive unmanned vehicles date back to the civil war where balloons carrying explosives were used in a combat role (Demir et al., 2015). Historically, much of the field research has been accomplished with the use of humans collecting samples in all aspects of the research. Autonomous vehicles, such as unmanned air vehicles (UAVs), unmanned surface vehicles (USVs), autonomous underwater vehicles (AUVs), and unmanned ground vehicles (UGVs) can help accomplish much of this research saving cost and keeping researchers out of harm's way all while reducing the environmental impact caused by field-based studies (JONES IV et al., 2006; Arifianto and Farhood, 2015). Using UVs can allow for extremely precise measurements in environments that are dangerous or inhospitable to humans (Weilin et al., 2003). These robots have the potential to stay on station for extremely long periods of time without the need of refueling or replenishment (Sarda et al., 2016). Likewise, they can cover extremely long distances without the need to rest and recover (Warren et al., 2016). In this

research, USVs and UAVs are used in situations where precision, repeatability and safety are needed which could be to difficult or practically impossible for manned operation. In the case of the UAVs used in part of this research, there were no practical manned alternatives to accomplish the required data collection (i.e. manned aircraft could not have safely and legally collected samples at the location and altitudes of sample collection). These UVs can accomplish tasks, that in the past may have considered to impractical for people to accomplish, opening new doors for research.

1.2 Objectives

The objective of this research is to identify and quantify the distribution and possible transport of microorganisms such as BBB below, near and above the AWI as well as map the flow of thermal energy at this interface. To achieve these objectives the following goals were identified: (1) develop the necessary autonomous platforms and integrate or design any necessary sensors to achieve the research objectives; (2) use these tools to study the thermal and biological transport at the AWI.

Objective 1: Map temperature profiles and resolve the boundary layer at the air/water interface (AWI) using high resolution distributed temperature sensing (HR-DTS) onboard an unmanned surface vehicle (USV)

Hypothesis 1: HR-DTS can be used onboard a USV to map temperature profiles of the AWI and to identify the boundary layer at the AWI.

Objective 2: Sample microbes from the water with a USV at multiple depths and locations

Hypothesis 2: The spatial distribution of microbes can be characterized in aqueous environments by sampling the water with a USV at multiple depths and locations.

Objective 3: Sample microbes from the atmosphere with a USV at the AWI

Hypothesis 3: The transport of microbes at the AWI can be characterized by monitoring particle sizes and collecting and culturing microbes from USV sampling missions.

Objective 4: Track and localize hazardous agents (tracer dyes) using a USV in aqueous environments.

Hypothesis 4: Agents can be tracked in water using a USV equipped with underwater sensors.

1.3 Attributions

Dr. David G. Schmale, III served as a co-advisor for this work. Dr. Schmale provided guidance on experimental design, planning, and writing for all the work presented here. He participated in all field research and was instrumental in the development of the FORES-PAsE sensor in chapter 2. He is listed as the corresponding author for Chapters 2, 3, 4, and 5.

Dr. Linsey C. Marr served as a co-advisor for this work. Dr. Marr provided guidance on experimental design, writing, and editing for Chapter 4.

Dr. Shane D. Ross served as a committee member and provided guidance throughout the completion of this dissertation.

Dr. John Little served as a committee member and provided guidance throughout the completion of this dissertation.

Regina Hanlon contributed to experimental design, planning, writing and was a field operator for work presented in Chapters 3, 4, and 5. She designed and performed the biological plating and ice-nucleation assays for work presented in Chapter 3 and 4.

Dr. Chad Higgins was instrumental in the design and development of the FORESPASE sensor and provided the supporting computer instrumentation for the work in Chapter 2. He contributed to experimental design, planning, writing and was a field operator and is listed as a co-author for Chapter 2.

Robert Predosa was instrumental in the design and development of the FORESPASE sensor in Chapter 2. He contributed to experimental design, planning, writing and was a field operator and is listed as a co-author for work presented in Chapter 2.

Dr. Hinrich Grothe served as a field operator in partial support of work presented in chapter 5.

Niki McMaster served as a field operator in partial support of work presented in chapter 4.

Chapter 2. Mobile distributed temperature sensing of the air-water interface of an aquatic environment with an unmanned surface vehicle

Craig W. Powers, Robert Predosa, Chad Higgins, David G. Schmale III*

Submitted: November 2017

To: Journal of Unmanned Vehicles

Status: Accepted November 2017

2.1 Abstract

Aquatic habitats have a boundary layer near the air-water interface (AWI) that governs mass transport. Little is known about temperature profiles and boundary layers at the AWI. We used a high-resolution distributed temperature sensing (HR-DTS) system onboard an unmanned surface vehicle (USV) to resolve temperature profiles from about 1 m above and 1 m below the surface of the water. Our USVHR-DTS system resolved a temperature differential of about 5.5°C at the AWI, spanning a distance of approximately 13 cm. DTS profiles were similar for stationary holds and forward and reverse transects in the water. There was a significant change in temperature as a function of height, with an exponential

decrease in temperature starting around 13 cm down to the AWI ($P = 2 \times 10^{-16}$). This is the first application of a HR-DTS onboard a USV to examine temperature profiles across the AWI. To our knowledge, these are the first high resolution temperature profiles of the AWI captured from a mobile platform. Because our USV-HR-DTS system is mobile, it could be used to profile temperatures at the AWI at multiple locations in a large body of water. This technology could also find unique applications in the measurement of meteorological drivers of hazardous agent dispersal for source localization efforts.

2.2 Introduction

Unmanned surface vehicles (USVs) have been used for a variety of dull, dirty, and dangerous missions, including monitoring of water temperature around nuclear power plants (Yuh et al., 2011) and measuring underwater volcanic activity (Dunbabin and Marques, 2012). USVs can be used to understand flow measurements in aquatic systems by tracking the movement of tracer dyes (Steimle and Hall, 2006). Understanding the environment and natural environmental processes is becoming increasingly important because of natural disasters and other environmental changes.

The majority of the Earths surface is covered with water, and the airwater interface (AWI) acts as the boundary between the atmosphere and the water. The AWI governs transport of material and energy between bodies of water and the atmosphere (Rashidi et al., 1991). The AWI has structural components that affect this transport, such as the cool-skin thermal boundary that exists in the atmosphere and is normally <1 mm thick (Handler et al., 2001). Particles of all types (including microbes) can become airborne if they can cross the AWI (Alpert et al., 2015). Some microbes that live and reproduce in water, such as Pseudomonas syringae, are known plant pathogens and may serve as drivers of precipitation processes

(Morris et al., 2008). Consequently, research is needed to understand the role of the AWI in heat transfer and aerosolization of abiotic and biotic particles.

Fiber optic cables that are used for telephones, internet, and cable television may also be used for environmental sensing in a technological application known as distributed temperature sensing (DTS) (Selker et al., 2006). DTS was originally developed for the oil and gas industry in the early 1980s (Kersey, 2000; Ukil et al., 2012). More recently, environmental scientists, hydrologists, and other natural scientists have appropriated this high-resolution technology for a range of applications in surface water, groundwater, and atmospheric science monitoring. The high spatial (1 cm) and temporal (1 Hz) resolution of DTS-derived temperature data can provide higher data resolution than conventional point-source measurements. This improved data density has helped to uncover hyporheic zone exchanges in streams, groundwater source flows, stream temperature profiles, and atmospheric boundary layer profiles (Briggs et al., 2012; Read et al., 2013; Bakker et al., 2015; Bond et al., 2015; Zeeman et al., 2015). DTS is possible because of the measurable scattering of light along a fiber optic cable at distances up to 30 km with a spatial resolution of 1 m and a temperature resolution of 0.01°C (Selker et al., 2006). DTS systems rely on Raman inelastic backscattering of incident light sent through a fiber optic cable. Two modes of backscattered light occur at any point along the fiber optic cable: (i) light scattered with resultant wavelengths shorter than the excitation light is called anti-Stokes scattering, $P_{as}(z)$; and (ii) light scattered with resultant wavelengths longer than the excitation light is called Stokes scattering, $P_s(z)$. Temperature is a known function of the ratio of Stokes to anti-Stokes backscatter intensity through the equation (Tyler et al., 2009; Selker et al., 2006):

$$T(z) = \gamma \left(ln \left(\frac{P_s(z)}{P_{as}(z)} \right) + C - \Delta\alpha \right)^{-1} \tag{2.1}$$

where gamma (γ), C, and alpha (α) are fitting parameters derived from a series of known, independently measured temperature values along the cable. $P_s(z)$ and $P_{as}(z)$ refer to the Stokes and anti-Stokes values, respectively. Figure 2.1 shows the physical calibration configuration used for our experiment (Hausner et al., 2011).

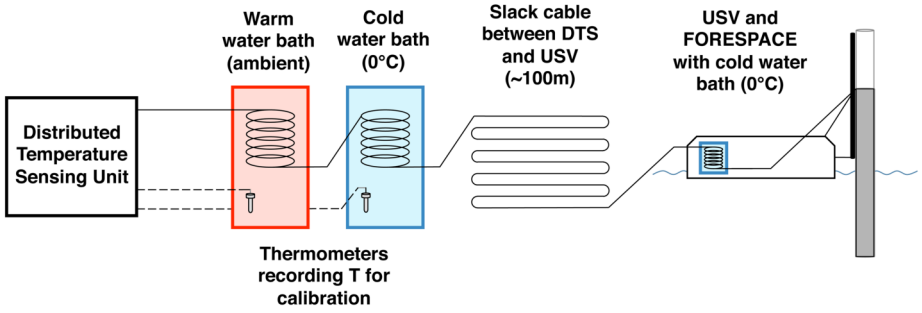

Figure 2.1: Configuration of our DTS system. The design includes a second cold-water bath onboard the USV (right) as a reference point to aid in locating the beginning of the usable data collected along the helical section.

Because the DTS system measures temperature wherever the fiber optic cable is placed, cable arrangements can be made to increase the spatial resolution. These arrangements are sometimes referred to as high-resolution distributed temperature sensing (HR-DTS) designs in which the fiber optic cable is coiled around a tube (Hilgersom et al. 2016). DTS and HR-DTS systems have been used to profile lake temperature (Vercauteren et al., 2011; Van Emmerik et al., 2013; Arnon et al., 2014b,a) at fixed (stationary) locations, and in both helical and regular cable configurations.

In this manuscript, we describe the development and field testing of a remotely operated HR-DTS system on board a USV: the fiber optic remote environmental sensing pipe for aqueous environments (FORESPASE). We hypothesized that DTS could be used to (i) map temperature profiles of the AWI while moving in an aqueous environment, and (ii) identify the

boundary layer at the AWI. To test these hypotheses, we developed a HR-DTS and deployed it on a USV to monitor temperature profiles in an aquatic system (a pond), and conducted field experiments to monitor temperature profiles under different sampling regimes (stationary holds, and forward and reverse transects). Robust unmanned marine systems have been developed for aquatic sensing and in particular, temperature measurement (Roberts and Sutton, 2006). Many of these systems focus only on a single point measurement (Ghani et al., 2014), some possibly varied spatially in a vertical profile (Cruz and Matos, 2010). Our work provides a high degree of spatial and temporal resolution of temperature measurements of the AWI and may be used to unleash a burgeoning field of aero-aquatic-ecology. This technology also has the potential to provide a mobile means of monitoring temperature gradients in the atmosphere, across land, and even through the water (Selker et al., 2006). Mobile HR-DTS could find unique applications and provide insights into the measurement of meteorological drivers of hazardous agents for source localization efforts.

2.3 Materials and Methods

2.3.1 USV

We used a Clearpath Robotics Kingfisher M200 USV (Clearpath Robotics, Kitchener, Ont., Canada). This electric USV weighs 28 kg, is 1.35 m × 0.98 m × 0.32 m (L × W × H), has a maximum payload of 10 kg, and can be operated via remote control or autonomously via an onboard computer. The removable 29 Ah batteries provided up to 3 h of continuous runtime. The two electric impeller thrusters allowed for a maximum speed of 1.7 ms^{-1} and provided steering via differential thrust. This configuration allowed for extremely precise, controlled movements and shallow operations with minimal disturbance to the surrounding

aquatic environment. The main chassis of the USV was made of aluminium, which has a high thermal coefficient (Touloukian et al., 1970) allowing for heat generated by the onboard computers to be distributed efficiently along the entire chassis. The chassis was thermally isolated from the water by two pontoons made of fiberglass, which also has a low thermal coefficient (Touloukian et al., 1971) helping to prevent heat transfer to the water.

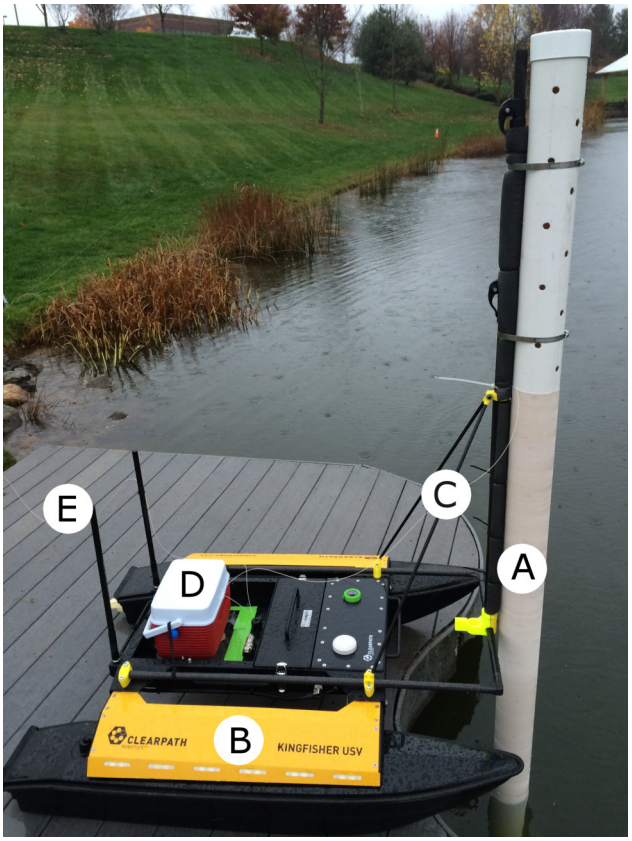

Figure 2.2: The FORESPASE (A) installed on the front of the USV (B). The coiled fiber optic cable extends about 1 m above and 1 m below the AWI when the USV is in water. After the pipe, the cable (C) was fed through a cooler (D) located to the rear of the USV before running (E) to the dock and into the FORESPASE computer. The cooler, which contained ice water, produced an inverted temperature spike in the data for calibration purposes.

2.3.2 Development and attachment of the FORESPASE

The FORESPASE system

The FORESPASE system consisted of a perforated PVC pipe of length 166.85 cm with an outside diameter of 10.76 cm, and wall thickness of 0.215 cm (Fig. 2.2). The pipe was wrapped with a 900 m, white-jacketed, multimode, fiber optic cable reinforced with aramid fibers (for tensile strength) by spinning the perforated PVC-pipe on a rotating mount along the longitudinal axis (cable was from www.AFLglobal.com; item, SX001509U601-BIF). To identify the exact location on the fiber where the beginning of usable measurements exists, a small cooler (ice bath) was placed at the rear of the boat (Fig. 2.2), in which the fiber was looped before leaving the boat and extending up the dock to the ground vehicle containing the DTS computer system. This computer captured the wavelengths of light from the fiber optic cable. The ice bath provided a reference temperature at a known location on the cable from which the beginning of the fiber-wrapped PVC pipe could be calculated. The FORESPASE system was mounted to the USV via carbon fiber tubing, well forward of the USV pontoons and chassis, to ensure that the temperature measurements would be free from thermal pollution created by the USV itself (Fig. 2.2). Additionally, the location of the FORESPASE system provided undisturbed access to the AWI.

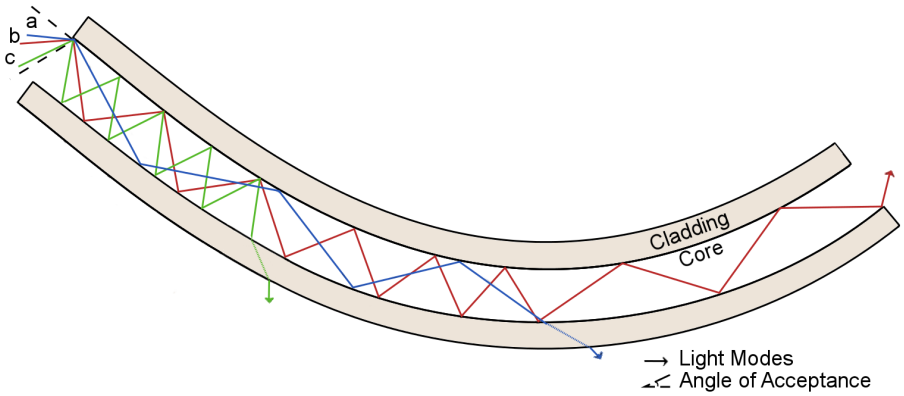

Figure 2.3: Angles of incidence for different modes of light. The more acute angle, mode c, correlates with the relatively short anti-Stokes backscatter wavelengths. The longer wavelength mode, mode a, has an angle of incidence that allows for it to successfully pass through the bend in the cable, again provided the radius of the bend is at least 10 cm. Diagram modified from Hilgersom et al. (2016).

Coil Diameter

While providing the possibility of unprecedented spatial resolution, helical configurations present a potential physical challenge that must be taken into account. If the radius of the coil is too tight, a disproportionately high number of anti-Stokes (shorter wave lengths) modes of light are lost (so-called differential attenuation), most notably in the first 100 m (Arnon et al., 2014b,a). There are two approaches to mitigate the resultant differential attenuation: post-processing of the signal return data, or preemptive experimental design if the scenario allows (for example, a helical configuration utilized in a small diameter borehole would require post-processing). Arnon et al. (2014b,a) developed a moving average method to correct for the differential attenuation that results from an undersized coiling diameter. Reliable temperature data were needed to confirm results of the empirical approach. Hilgersom et al. (2016) found that a minimum coil diameter of 10 cm is needed to physically mitigate the issue of differential attenuation, though this was dependent on the cables index type (Fig. 2.3). We constructed our HR-DTS pipe with a coil diameter of 10.76 cm, just beyond the

minimum stated diameter of the coil sufficient to avoid differential attenuation.

Solar Radiations Effect on Temperature Readouts

Direct solar radiation, also known as solar loading, can impact the measured temperatures provided by the DTS instrument. Solar loading is of particular importance for atmospheric applications because of the thermal properties of air. Poor experimental design can lead to conditions where solar radiation forces the cables physical temperature to be higher than the surrounding air (De Jong et al., 2015). There are four approaches to mitigate the impact of solar loading: do not perform experiments in direct sunlight, use small-diameter fiber optic cable to reduce surface area, use a white-jacketed fiber optic cable (Selker et al., 2006), or perform temperature corrections as outlined by De Jong et al. (2015). Note that a second, larger (or smaller) diameter cable is required to perform de Jongs correction. We performed our measurements on a fully overcast day at sunset with a 900 μm, white-jacketed, bend-insensitive fiber optic cable. These sensor component choices and experimental design considerations contributed to the reduction in the total influence of solar radiation on temperature readings. Future analysis of the effect of sunlight on the fiber optic cable during clear days is needed to validate the DTS system for use in all weather conditions.

Spatial and Temporal Resolution Considerations

There is a difference in the reportable, true spatial resolution of a DTS instrument and the manufacturers designed resolution. The manufacturer of the DTS system we used specified a spatial resolution of 12.5 cm, which is an accurate reflection of our devices ability to read temperature, but it does not imply that the device can account completely for a steep change in temperature between two adjacent locations along the cable (Tyler et al., 2009).

The distance along the cable needed to resolve 90% of the change in two independently known temperatures increases beyond the manufacturers stated, readable, spatial resolution (Tyler et al., 2009). For our experiment, this resolution consideration is mitigated by the sequential data points along the cable (28 per 1 cm of vertical resolution).

2.3.3 Study site and design

The study site was a small pond located on the campus of Virginia Techs Corporate Research Center in Blacksburg, Va., USA. The triangular-shaped pond has an approximate surface area of 3000 m^2. A small dock (Fig. 2.4; N37°11′56.0″; W8°0;24;33.2) was used as a base of operations for launch and recovery of the USV. The pilot in command (PIC, Powers) controlled the USV from the area immediately behind the dock. The fiber optic cable was fed to the USV from an individual (Higgins) standing on the dock, and ran up the hill west of the sampling location to a ground vehicle containing the DTS computer system. Because of the tethered nature of the system, remote-controlled operation was used for all missions (i.e., autonomous control of the vehicle would not have been feasible with the tethered configuration, because the individual managing the cable was in constant contact with the PIC during each mission). The use of onboard compact components, in place of the remote DTS computer system, would allow for full autonomous operation of the FORESPASE system in the future. Such a system could be used to monitor temperature in highly radioactive environments (Yuh et al., 2011), where the use of manned boats would be considered risky or dangerous.

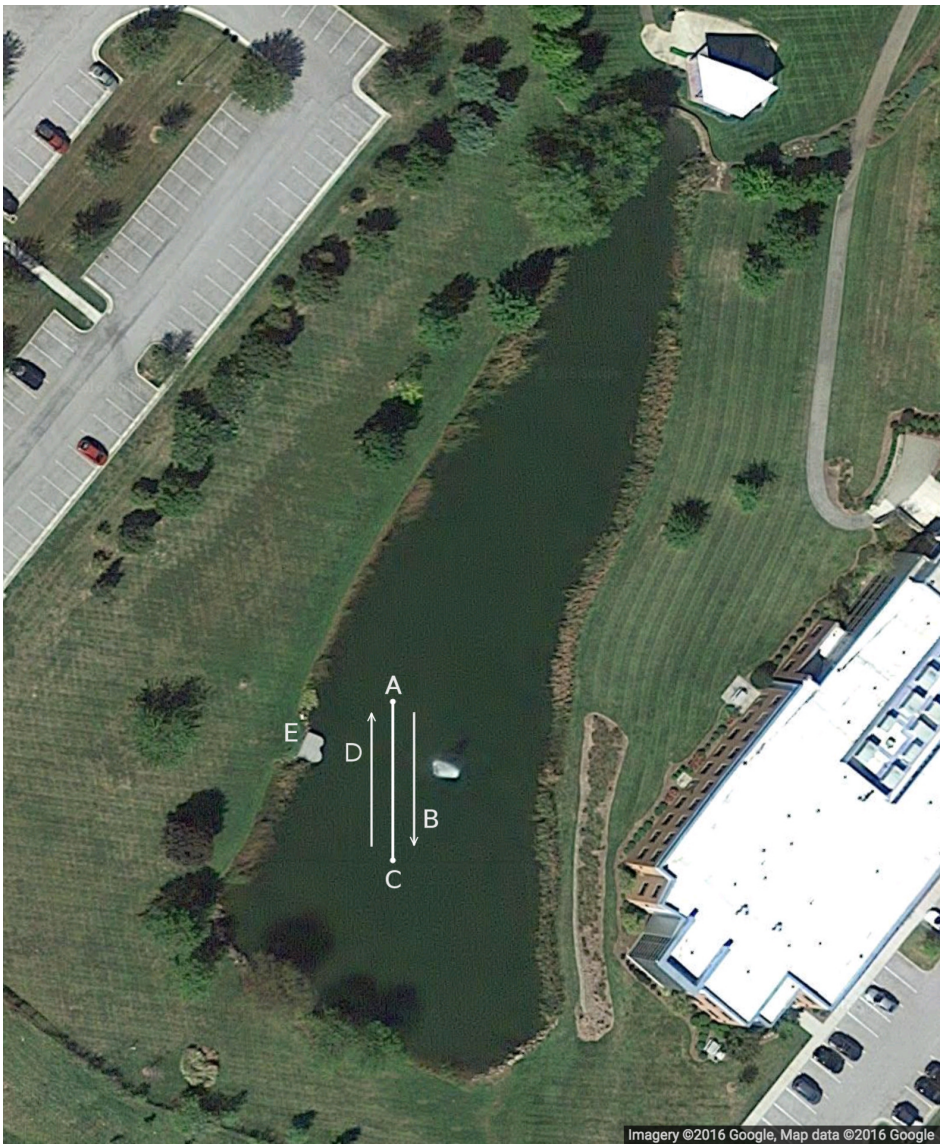

Figure 2.4: Map of the field experiment site in Blacksburg, Va., USA. Figure 2.4 shows the pond and the respective treatments (A, B, C, and D), each of which consisted of eight replicates. Treatment A was a hold north position, treatment B was a forward transect, treatment C was a hold south position, and treatment D was reverse transect. The USV and fiber cable management were coordinated on a small dock at the waters edge (E). For each treatment, the HR-DTS system recorded data spanning the AWI at 1 Hz for 1 min.

Four treatments were used to capture the vertical temperature gradient across the air water boundary (hold north position, forward transect, hold south position, and reverse transect) (Fig. 2.4). A continuous cycle of holding and transecting between holding positions was orchestrated for a total of eight repetitions for each treatment. For each treatment, the temperature measurements were recorded for approximately 1 min giving a total of 32 measurements. During the study, because of the lack of wind and any water-based cur rents, the USV did not require any thrust corrections to hold position for the two stationary points (Fig. 2.4). For the two transect movements, the throttle setting was held at a constant 0.34 m s^{-1}. Visual landmarks were used to guide and hold the USV repetitively over the course of all measurements. The distance from the PIC to the USV (Fig. 2.4, E) was around 10 m for all measurements, minimizing potential deviation from planned path transects. The objective of this study was to test the reliability of the FORESPASE system at making temperature measurements of the AWI during both stationary holds and during moving transects.

2.3.4 DTS system

The DTS system used was the Silixa Ultima S (Silixa Ltd, Hertfordshire, UK). Maximum mechanical spatial and temporal resolutions obtained with this device were 12.5 cm and 1 Hz, respectively. Raman backscattered information was initially converted to temperature utilizing a software package developed by Center for Transformative Environmental Monitoring Programs (CTEMPs), an environmental research support center from Oregon State University and the University of Nevada-Reno (www.ctemps.org), based on the procedures outlined in (Hausner et al., 2011).

2.3.5 Missions

We conducted 32 sampling missions with the FORESPASE system. Eight of these missions were a north stationary hold, eight were a south stationary hold, eight were forward transects, and eight were reverse transects. During these sampling missions, the USV was

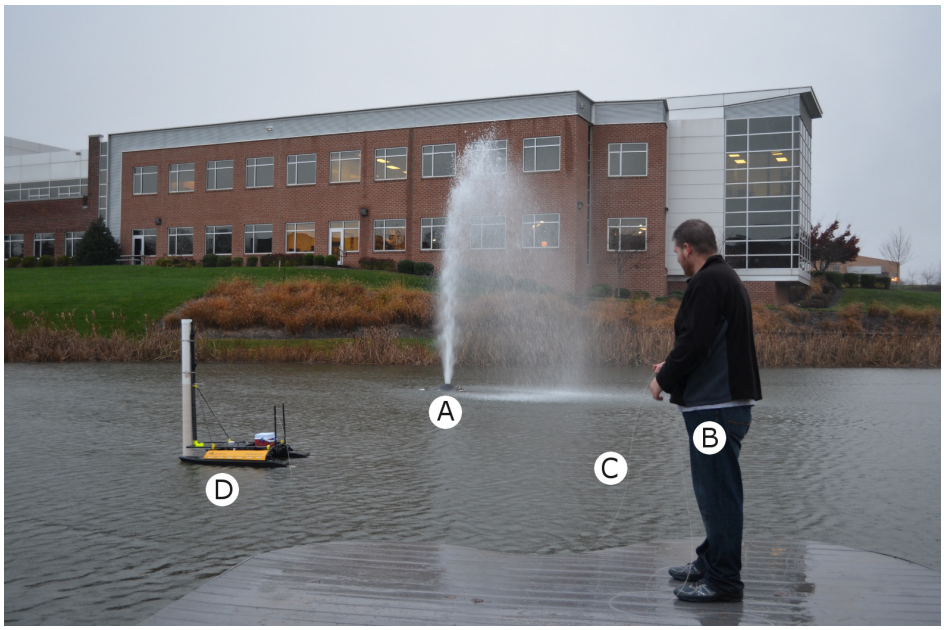

Figure 2.5: A transect maneuver (treatment D) from the south hold to north hold position passing a small fountain (A). Higgins (B) managed the DTS fiber optic cable (C) leaving the USV (D) to the computer in the command vehicle. In future operations of the FORESPASE system onboard larger USVs, the DTS computer could be housed onboard the USV without any need for cable management.

operated by the PIC (Powers) using remote control, while the cable was manually fed to the USV by another individual (Higgins) on the dock (Fig. 2.5). The manual handling of the fiber optic cable from the DTS system was needed to prevent damage to the cable and potential entanglement in the USV. The pond was small enough that visual landmarks (e.g., a fountain shown in Fig. 2.5) sufficed to keep the USV on the pre-planned mission path. Winds were not a factor in the manual control and position holding of the USV. A constant, light rain event was occurring during the entire study, which provided an additional mitigation factor

for the solar loading issue inherent with cable deployments in the atmosphere, as discussed previously.

2.3.6 Statistical analyses

Statistical analyses were conducted using the R language. An analysis of covariance (ANCOVA) was performed after verifying the residuals of the data were approximately normally distributed for data below, at, and above the AWI.

2.4 Results

2.4.1 Results of statistical analyses

There was no significant difference in temperature between treatments for zones 1 (below the water) and 2 (at the AWI), but there was a significant difference for zone 3 (above the water) (Fig. 2.6; Table 2.1). This can be seen in the shift in the temperature range across the four treatments (Fig. 2.6). This correlation was found across each individual treatment including stationary treatments and was likely due to the change in atmospheric temperature during the study. There was a significant difference in temperature for change in depth for all three zones (Table 2.1). Zone 2 had a change of temperature of about 5.5 °C for a change of about 13 cm in height (Fig. 2.7), including the cool-skin range ($P = 2 \times 10^{-16}$).

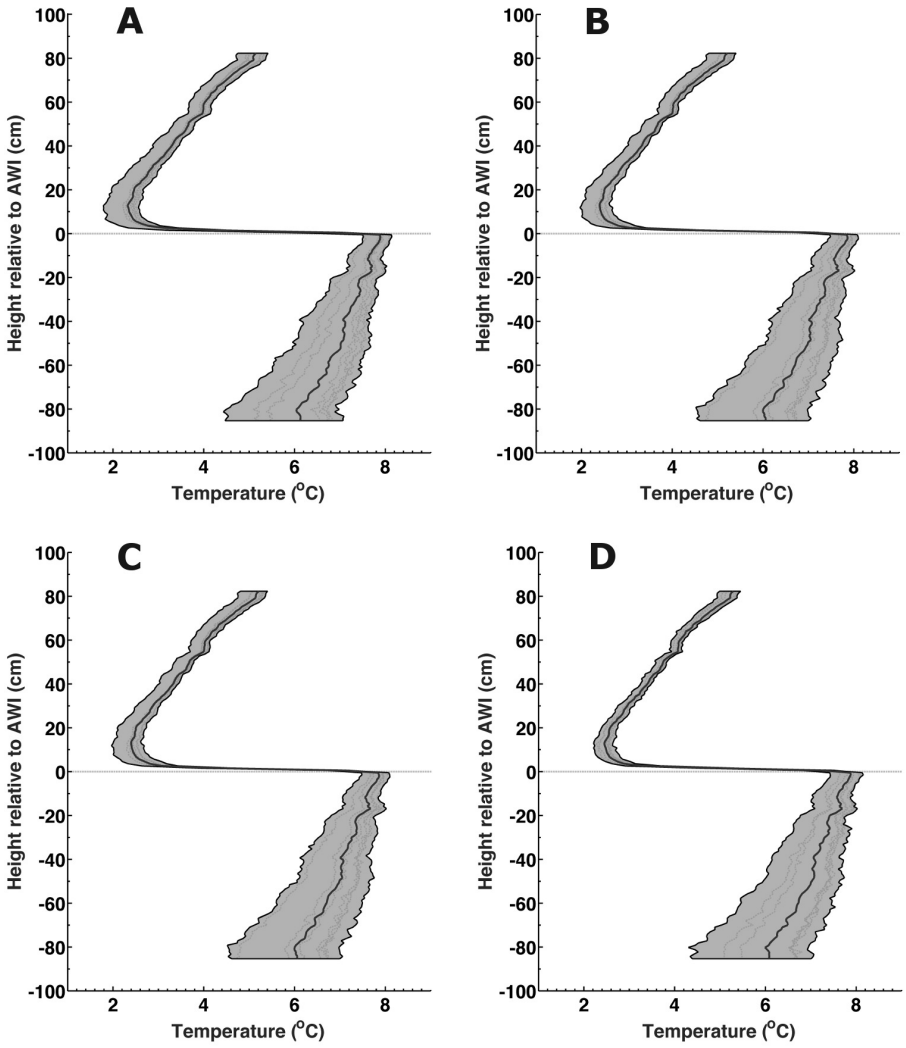

Figure 2.6: Each of the four treatments, hold north (A), forword transect (B), hold south (C), and reverse transect (D) with all measured temperature points from the eight repetitions in grey. The averaged temperature profile for each treatment is represented by a black line. No significant temperature variation was found across the four treatments at the set vertical resolution of 1 cm.

Table 2.1: ANCOVA results from analyzing the effect of treatment on temperature for the three zones; Zone 3 (above the water), Zone 2 (at the air water interface), and Zone 1 (below the water).

Response: Temperature	P - value
Zone 3	
Depth	< 2.2e-16
Treatment	< 2.2e-16
Zone 2	
Depth	< 2.2e-16
Treatment	0.2973
Zone 1	
Depth	< 2.2e-16
Treatment	0.1511

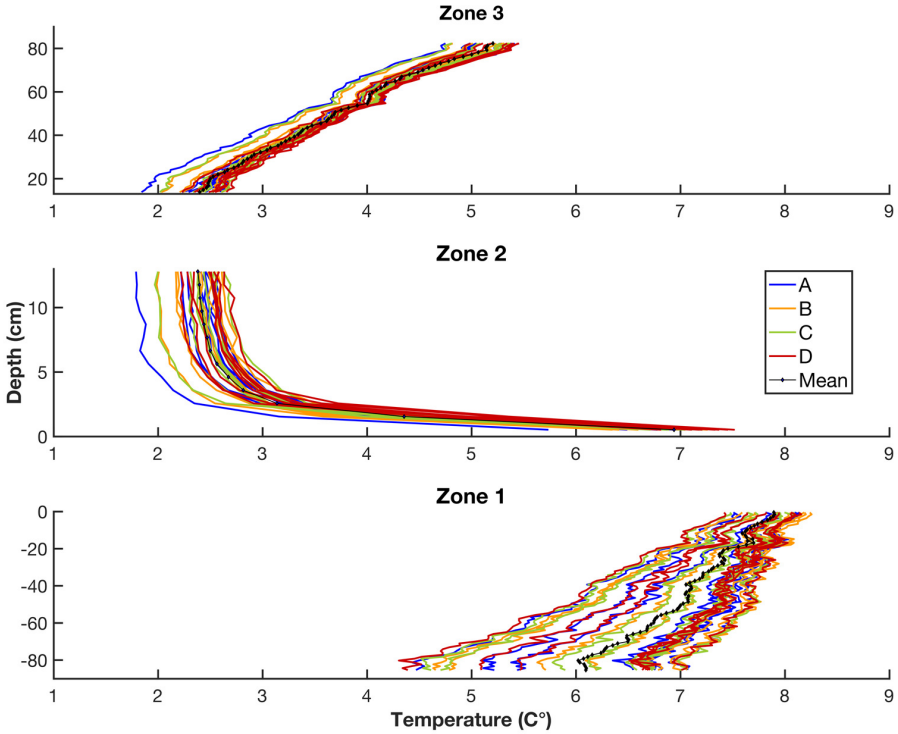

Figure 2.7: The three zones, the top (zone 3) from about 83 cm above the water surface to 13 cm above the AWI, the middle (zone 2) from 13 cm above the water surface to the AWI, and the bottom (zone 1), from the AWI to about 85 cm below the water surface showing the temperature variation over the eight replicates.

2.4.2 Observations of the boundary layer at the AWI

The initial plots of temperature profiles gathered show a well-mixed surface layer of air at the AWI (Fig. 2.6). The initiation of a temperature increase with height at approximately the first 510 cm above the water surface signifies this phenomenon (Fig. 2.7). To our knowledge, these are the first high-resolution temperature profiles of the AWI captured from a mobile platform that display this temperature phenomenon.

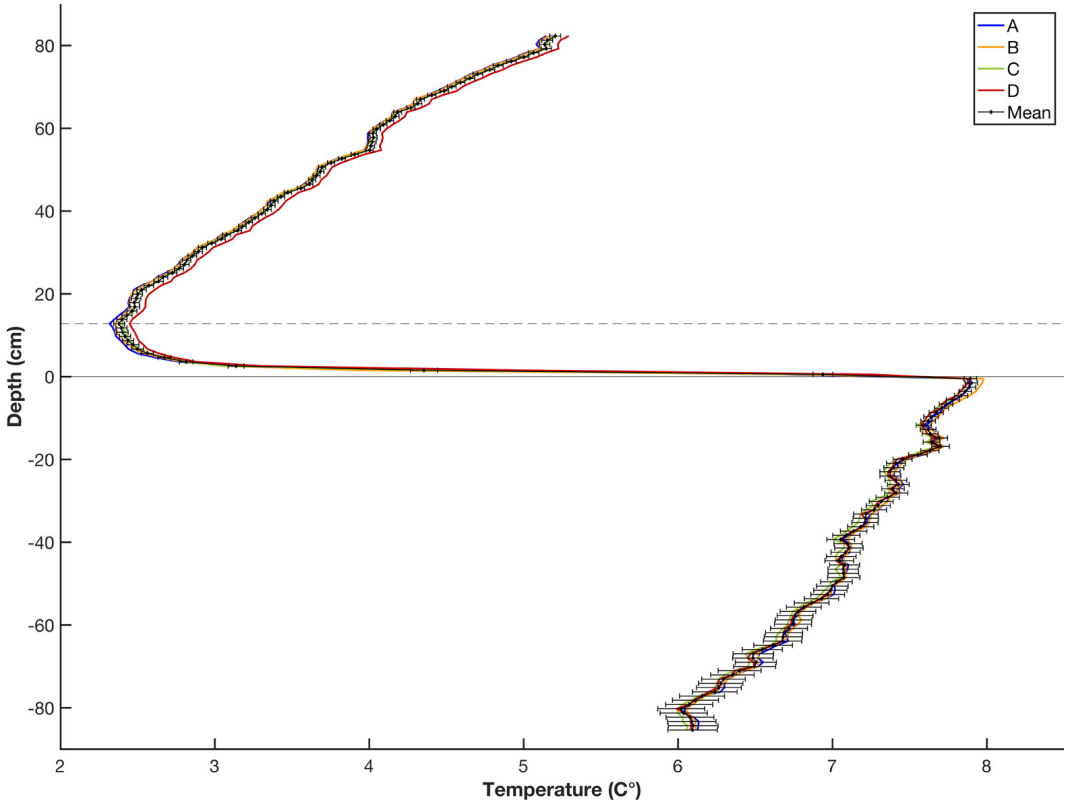

Figure 2.8: The mean for the four treatments (A, B, C, and D) with an overall mean and standard error of the mean (error bars). The solid horizontal line represents the AWI with temperature measurements below the AWI (zone 1) above to the dotted line (zone 2), and above the dotted line (zone 3).

2.4.3 Stability considerations

Zones 1 and 3 were statically stable. Relatively warm material was above colder regions with vertical gradients on the order of -3.6 °C m^{-1} in the air and 1.9 °C m^{-1} in the water. Zone 2 was statically unstable. That is, the water surface was warmer than the air immediately above. The thermal gradient (resolved by more than 10 points, see Fig. 2.8) in this parcel is extreme, on the order of 100 °C m^{-1}.

2.5 Discussion

We developed and implemented a unique HR-DTS system onboard an USV to provide an unprecedented resolution of temperature profiles from approximately 1 m below the surface of the water to approximately 1 m above the surface. To our knowledge, this is the first application of a mobile HR-DTS system (and the first using a USV) to examine temperature profiles across the AWI. HR-DTS can be used to gather temperature profiles in many different environments. As a static application, HR-DTS has been used to profile engineered shallow thermohaline lakes (Suárez et al., 2011), and could be used to monitor the thermohaline circulation that effects the warming of Europe (Latif et al., 2006). Likewise, seasonal changes in lake thermoclines could be monitored, and in these cases, spatial and temperature resolution requirements would be met by using HR-DTS. A mobile HR-DTS system, such as FORESPASE, could provide extraordinary detail while solving some deficiencies with other instruments, such as the expendable bathythermographs (XBTs), where temperature measurements from the top 34 m, the location of the AWI, can be unreliable due to the use of a thermistor (Fiedler, 2010). When conditions permit the use of a DTS compared to a traditional XBT, spatial resolution can be upwards of five times more accurate, and orders of magnitude more resolved (Narayanan and Lilly, 1993).

Our FORESPASE system resolved a temperature differential of about 5.5 °C at the AWI, spanning a distance of approximately 13 cm with a vertical resolution of 1 cm (28 cable sub-samples were aggregated to achieve a vertical resolution of 1 cm). Many transport structures, such as the temperature inversion we observed at the AWI, are smaller than existing measurement technology, such as XBTs can resolve (Narayanan and Lilly, 1993). To study these fine-scale structures, a tool like the HR-DTS is necessary. Unstably stratified air, namely, the air in zone 2, contains potential energy and can rise, unrestricted, to the zone immediately above. Thus, this zone is not expected to persist from an analysis of the buoyant stratification. Further study is needed to determine the mechanism by which this layer persists. These detailed measurements can be used to modify and verify existing models that exclude these important, but understudied, fine-scale structures.

The impact of potential external thermal sources, such as solar radiation and onboard computers and propulsion systems on the USV, should be considered for future mobile HR-DTS missions. Though our experiments were conducted during overcast conditions, operations during sunny days could be influenced by increased solar radiation. De Jong et al. (2015) used a system of two different-diameter fiber optic cables to estimate the temperature of a zero-diameter cable. The use of a zero diameter cable could improve the accuracy of temperature measurements under solar loading conditions. Additional methods to understand solar loading could consist of separate, independent sensors to measure temperature and solar radiation at different heights above the water surface. Though the placement of our HR-DTS system on the front of the USV was expected to minimize potential interactions with thermal sources onboard the USV (e.g., the onboard computers and the propulsion system in the back of each of the pontoons), these sources could potentially influence DTS measurements under extreme operating conditions (e.g., full throttle operation and high daily temperatures with increased solar radiation). Consequently, in the future, controlled experiments to quantify

the thermal contribution of the USV used to deploy HR-DTS systems are warranted.

DTS profiles were similar for stationary holds and moving transects in the water; there was no significant change in temperature across all four treatments ($P = 0.82$). These results indicate that transect measurements were not significantly affected by the speeds utilized by the USV in our study. Thus, the FORESPASE configuration could be employed in much larger bodies of water over larger temporal scales. By placing the FORESPASE software and hardware onboard the USV, it would be possible to overcome the tethered nature of the USV. There are some obstacles to overcome in such a scenario, such as decreased endurance of the USV. In such a case, where endurance is needed for much larger scales of operation, a large USV with payloads in the tens to hundreds of kilograms (e.g., a full-scale watercraft) could allow complete autonomous operation. Coupled with other emerging technological advances in sensor technology and multiple coordinated robots, this configuration could produce detailed maps of the Earths surface waters and related structures. There was a significant change in temperature as a function of height with a decrease in temperature, starting around 13 cm down to the AWI ($P = 2 \times 10^{-16}$). The cool skin, which is normally <1 mm (Handler et al., 2001), may have been displaced and stretched because of the light rainfall that occurred during our study. Temperature accuracy was less precise at depth in the water. This was likely due to the normal attenuation of the DTS signal with respect to distance from the device. Total cable length was approximately 750 m, which cor- relates with an expected accuracy loss over that distance with the given fiber type. Further studies could inform what role the rain played on the AWI and zone 2. For example, studies conducted at different times of the day, different seasons, and different weather events (such as snowfall) will clarify in detail the daily to yearly thermodynamic processes happening in the pond. Based on the data, it should be possible to model the heat capacity and flux of the pond and of the precipitation entering the pond. Utilizing this information would

make it possible to better understand the heat flux across the AWI, and more accurate models could be developed to predict the changing thermal properties of the AWI in other systems. This could lead to a better understanding of many other aquatic and meteorological systems involved with AWI transport, such as the thermohaline circulation, which affects the warming of northern Europe (Manabe et al., 1991).

Oceans and lakes represent the majority of the surface area and about half of the primary biomass production of the planet (Alpert et al., 2015). The AWI is the boundary between the world of aquatic and the ecological domain we live in. As such, it governs the emission of this biomass, some via aerosolization, into the atmosphere. Some of the aerosolized biomass may be microorganisms that threaten plant health (Morris et al., 2008), and an increased understanding of the role of the AWI in this process is needed to plan for and mitigate the spread of these pathogens.

Our work provides an acute resolution of temperature measurements of the AWI and may be used to unleash a burgeoning field of aero-aquatic-ecology, with broader impacts on oceanography and meteorology. One could imagine a small fleet of autonomous USVs, utilizing HR-DTS technology, and traversing the worlds oceans and lakes collecting and uploading this data via satellite links. Such data would lead to a better understanding of our environment in a changing climate.

2.6 Acknowledgements

This work was supported in part by seed grants to D. Schmale from the Institute of Critical Technology and Applied Science (ICTAS) (Grant Number 176025, Environmental Sensing of the Atmosphere and Water with Fiber Optic Lines) and the College of Agriculture and Life Sciences at Virginia Tech. DTS instrumentation was provided by and supported by the

Center for Transformative Environmental Monitoring Programs at Oregon State University.

Chapter 3. Remote collection of microorganisms at two depths in a freshwater lake using an unmanned surface vehicle (USV)

Craig W. Powers, Regina Hanlon, David G. Schmale III*

Submitted: October 31 2017

To: PeerJ

Status: In review

3.1 Abstract

Microorganisms are ubiquitous in freshwater aquatic environments, but little is known about their abundance, diversity, and transport. We designed and deployed a remote-operated water-sampling system onboard an unmanned surface vehicle (USV, a remote-controlled boat) to collect and characterize microbes in a freshwater lake in Virginia, USA. The USV collected water samples simultaneously at 5 and 50 cm below the surface of the water at three separate locations over three days in October, 2016. These samples were plated on a non-selective medium (TSA) and on a medium selective for the genus Pseudomonas (KBC) to estimate concentrations of culturable bacteria in the lake. Mean concentrations ranged from

134 to 407 CFU/mL for microbes cultured on TSA, and from 2 to 8 CFU/mL for microbes cultured on KBC. There was a significant difference in the concentration of microbes cultured on KBC across three sampling locations in the lake (P = 0.027), suggesting an uneven distribution of Pseudomonas across the locations sampled. There was also a significant difference in concentrations of microbes cultured on TSA across the three sampling days (P = 0.038), demonstrating daily fluctuations in concentrations of culturable bacteria. There was no significant difference in concentrations of microbes cultured on TSA (P = 0.707) and KBC (P = 0.641) across the two depths sampled, suggesting microorganisms were well-mixed between 5 and 50 cm below the surface of the water. About 1 percent (7/720) of the colonies recovered across all four sampling missions were ice nucleation active (ice+) at temperatures warmer than -10°C. Our work extends traditional manned observations of aquatic environments to unmanned systems, and highlights the potential for USVs to understand the distribution and diversity of microbes within and above freshwater aquatic environments.

3.2 Introduction

The ecology of freshwater ecosystems is linked to the temporal and spatial dynamics of aquatic microorganisms (Beisner et al., 2006). Microorganisms play an important role in the food web as drivers and indicators of ecosystem health (Newton et al., 2011; Shafi et al., 2015). Biological ice nucleators such as Pseudomonas syringae have been collected throughout the water cycle, and have been implicated as drivers of precipitation processes (Ichinose et al., 2013; Morris et al., 2008). New research is needed to understand and predict the abundance, distribution, and diversity of microorganisms in freshwater lakes (Morris et al., 2008). Humayoun et al. (2003) observed differences in microbial diversity at different

depths in Mono Lake, California, USA. Song et al. (2007) examined distributions of toxins from algal blooms along the water column in Lake Taihu, Wuxi, China. Pietsch et al. (2017) reported high concentrations of P. syringae in Claytor Lake, VA, USA from the surface down to almost 10 m. These authors also showed that concentrations of P. syringae varied dramatically from day to day and location to location (Pietsch et al., 2017). Though these observations have provided important data on the distribution of microorganisms in aquatic environments, they have been limited by manned collections (i.e., at least one human was needed to collect the samples). In this study, we extend these manned observations to unmanned systems, highlighting the potential for robots to collect samples to study the distribution and diversity of microbes within and above freshwater aquatic environments allowing for precise and repeatable measurements.

Recent advances in unmanned systems have created new possibilities for sampling natural and managed ecosystems (Pennington et al., 2016). Though these unmanned systems are seeing increased use in a variety of scientific applications, many challenges must be overcome. First, long-range control and communication of unmanned systems require high data rates, often more than satellite-based communication can provide. Commercial Wi-Fi systems are one potential solution to fill this need (Takahata et al., 2016). Such systems have been used for surface communication in autonomous underwater vehicles with a range of 1 km (Stokey et al., 2005), and in specialized point to point sustained networks at ranges of over 100 km (Flickenger et al., 2008). Second, object avoidance is an extremely important aspect of unmanned operations and becomes an absolute requirement when operating in existing complex manned boat traffic. Adaptive evaluation schemes and algorithms have been recently developed and tested to allow autonomous watercraft to meet international regulations for preventing collisions at sea (Kuwata et al., 2014; Shah et al., 2016).

In this manuscript, we describe the development and deployment of a USV to sample water

remotely at multiple depths and locations in a freshwater lake. This integrated system was used to test the hypothesis that concentrations of microorganisms in Claytor Lake, VA vary with depth, geographic location, and date of sampling. The specific objectives of this work were to (1) develop an automated water sampler to remotely collect samples of water with a USV in a freshwater lake, (2) conduct a series of field experiments to remotely collect samples of water with the USV at two depths at three different locations in the lake, and (3) culture microorganisms from the water samples on a non-selective medium (TSA) and on a medium selective for the genus Pseudomonas (KBC) to estimate concentrations of culturable bacteria in the lake. Our work represents a unique approach to collect and characterize the distribution of microorganisms in aquatic environments, and could be extended to the tracking the movement of hazardous agents during algal blooms and in floodwaters generated by hurricanes and other extreme weather events. .

3.3 Materials and Methods

3.3.1 Study site and design

Samples were collected over three consecutive days on 25, 26, and 27 October, 2016 in Claytor Lake, VA, USA. This freshwater lake has an approximate surface area of 18.2 square kilometers. Samples were collected in a cove located at N37°2.34′4″ W80°37.7′9″. The cove was selected in part due to its isolation; no manned boats (other than our pontoon boat used as our base station) visited the cove before or during our sampling operations. Water samples were collected at two depths (5 and 50 cm) below the water surface for three locations, L1 (N37°2.33′4″ W80°37.06′6″), L2 (N37°2.30′5″ W80°37.07′7″), and L3 (N37°2.35′9″ W80°37.12′4″) (Figure 3.1). Depths of the lake at each of the sampling locations were mea-

sured with portable sonar sensor (Signstek FF-003). The sensor was placed 20 cm below the surface of the water, and the depth reader output screen was monitored until the continuous reading on the screen did not vary more than 0.5 m for 10 readings. Depths for each of the locations were measured at 11 m for L1, 10 m for L2, and 4 m for L3. Sampling dates, times, and locations are provided in Table 1. Each location was separated by the transition time of the USV between each location. GPS coordinates were recorded for all navigation paths and each sample location (Figure 3.1). Though water temperature is an environmental variable, it was assumed to be constant across the distances and times within and among sample collections in this study.

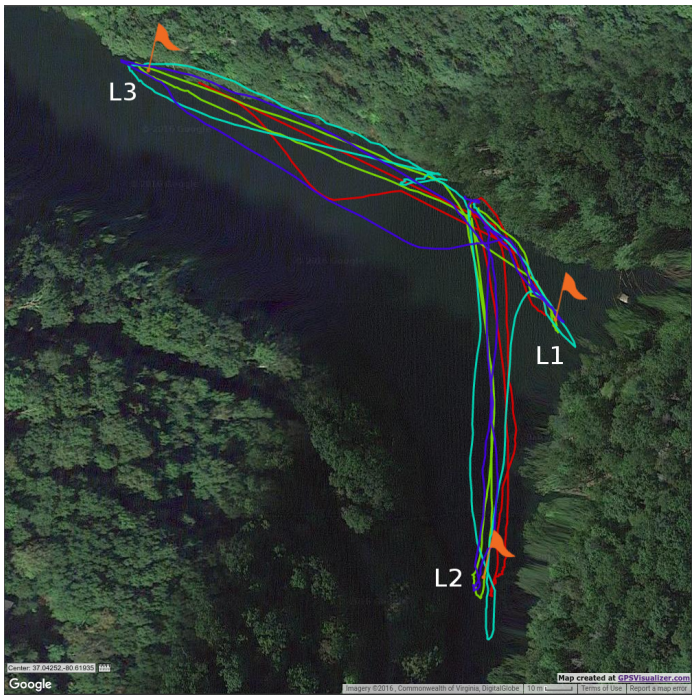

Figure 3.1: Unmanned surface vehicle (USV) navigation routes (Mission 1, red, Mission 2, green, Mission 3, cyan, and Mission 4, blue) and sample locations L1, L2, and L3 (orange flags) for the four missions conducted from October 25th to October 27th. The USV collected 500 mL of water from at two depths (5cm and 50cm) for each location. Map data: Google, Commonwealth of Virginia, DigitalGlobe.

3.3.2 Unmanned surface vehicle (USV)

A Clearpath Robotics Kingfisher USV (Clearpath Robotics, Kitchener, Ontario, Canada) (Figure 3.2) was used as our water-sampling platform. This electric USV weighed 28 kg, was 1.35 m x 0.98 m x 0.32 m (L×W×H), had a maximum payload of 10 kg, and was operated via remote control (the vehicle is equipped with autonomous navigation through a ground control station, but this was not used during our mission because of limitations with obtaining consistent GPS signals within the cove of interest). Each removable 29 Ah battery provided up to 3 hours of continuous runtime. Differential thrust provided steering via the two impeller thrusters and allowed for a maximum speed of 1.7 m/s. This platform enabled extremely precise, controlled movements in shallow waters and also minimized water disturbances to the surrounding aquatic environment that could be caused by the vehicle.

Figure 3.2: The Clearpath Robotics Kingfisher USV equipped with the automated water sampler on Claytor Lake, VA, USA. The water sampler onboard the USV collected samples of water at two different depths. Each sample was collected into sterile 1 L bottles. The operation of the vacuum pumps and sampling tubes were remote-controlled through a microcontroller and supporting electronics housed in a waterproof box. A collection bottle containing 500 mL of sterile water was used as an unexposed control during each mission. Image courtesy of D. Schmale.

3.3.3 Development of an automated water sampler onboard a USV

A water sampler was developed for deployment on a USV with the goal of sampling at two distinct depths for three locations (Figure 3.3). A vacuum system and flow rate was used to maximize the water collection rate while minimizing turbulent fluid flow at the collection nozzle. Seven 1 L bottles were used as the collection vessels. Two were used at each sampling location, with each of the bottles holding a sample from each of the two depths (5 and 50 cm). One bottle was used as a control (no sample). Each bottle was attached via Tygon B-44-4X PVC 1/4 ID, 3/8 OD tubing to an air pump (ZT370-01, Dongguan Zhentian precision electronic co., LTD, Dongguan city, Guangdong province, China.) calibrated to pull approximately 0.5 Lpm. Each bottle had a section of this tubing attached to a stainless steel tube that served to siphon the water directly from the lake. Six changeable siphons (one for each depth at each of three sampling locations) were attached to arms on the water sampler platform via 3D printed bevel gears (Supplemental File 1) that where actuated by waterproof servos (SX401WP, Hobbico Inc., Champaign, Illinois, USA). Two lengths of stainless steel tube were chosen to allow for simultaneous collections at depths of 5 and 50 cm for each location. The tubing ends were bent into slight curves so that a water trap existed while the tubes were in the horizontal, stowed position (Figure 3.2). Aliquots of 10 mL of sterilized water were placed into each of the six tubing water traps to act as an environmental seal to prevent air flow movement and contamination of the sampling tube while the USV proceeded through the sampling cycle. At the start of the collection cycle at each location, one sampler arm transitioned from a rear horizontal stowed position into the water, then past the vertical position and to a forward horizontal position, 175 degrees from the starting position, in order for the sterilized water to flow out of the tubing. This cleared the line of sterile water preparing the system for water collection. The arm then transitioned back into the water to a vertical position. Approximately 500 mL of water was

then siphoned simultaneously for both depths into a collection bottle for each depth. The arm then transitioned back to the horizontal stowed position where water in the tubing (leftover from the collection process) would stay in the water trap at the end of the tubing. This water served to prevent contamination from the air while the USV completed the collection cycle. The stainless steel tubing was disinfested with ethanol and flushed with sterile water after each sampling day, and on the last day sterile water was used to flush the tubing between the two sampling periods for that day. A microcontroller (keyestudio MEGA 2560, Chang Yong Rd., Longhua New District, Shenzhen, China) in conjunction with servo and motor driver circuits, were integrated into the water sampler and USV to control motion and timing of the servos and pumps. The microcontroller was then controlled through the computer on the USV via a wireless link to a portable computer running a Linux operating system.

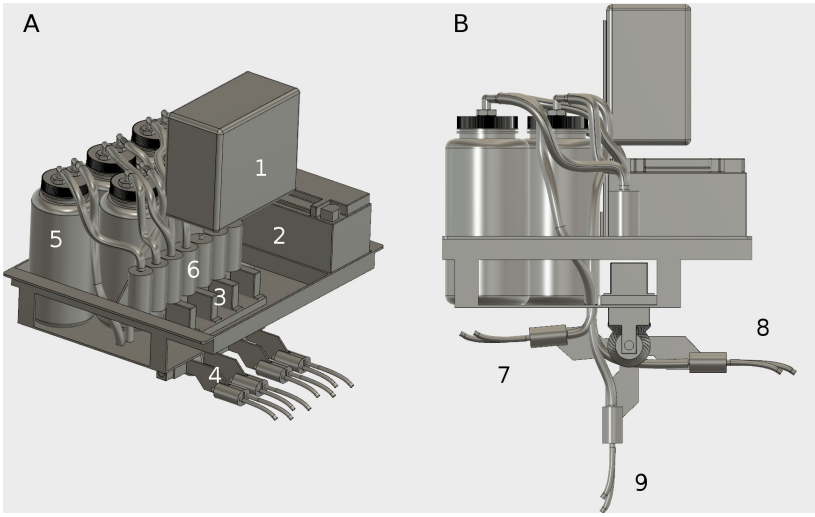

Figure 3.3: Engineering design of the automated water sampler onboard the USV. The sampler (A) consisted of a microcontroller and electronics (1) powered by a lithium iron phosphate battery (2) that actuated servos (3) to control siphon positions (4) and pump water into 1 L containers (5) with vacuum pumps (6). During vehicle movement, the siphon arms (B) were in the stowed configuration (7). Upon reaching the sampling location, the appropriate arm rotated 175 degrees (8) to allow the sterile water in the tube to flow out. The arm then rotated back 90 degrees (9) into the water for collection. After a set amount of collection time, the arm returned to the stowed configuration (7) before proceeding to the next location.

3.3.4 Processing of Samples for Culturable Bacteria

After the return of the USV from each collection cycle, the lake water samples were removed from the USV and capped with sterilized screw cap lids. After all collections for the day were completed, samples were transported on ice in a cooler to the lab for processing in the same 1 L collection bottle (Nalgene #2187-0032). Subsamples of 250 mL from each collection bottle were filtered through a 47 mm diameter, 0.22 mm GSWP nitrocellulose filter (Millipore#9004-70-0) in a sterile holder and receiver unit (Thomas #300-4100). Filters were transferred to sterile 100 mL bottles with 5 mL of the filtrate and a stir bar. Samples were stirred for 10 min to resuspend microorganisms from the filter surface (resulting in a 50X concentration). A 0.5 dilution of this resuspension (25X concentration) was used for plating. Kings B medium plus cycloheximide (KBC), a medium semi-selective for Pseudomonas (Mohan et al., 1987), was used to plate 200 μL of both the 25X and 50X concentrations in triplicate. This medium consisted of 15 g/L proteose peptone, 1.5 g/L anhydrous K2HPO4, 10 mL/L 100% glycerol, 6 mM MgSO4 with 24 mM H3BO3, cephalexin (10 mg/L), and cycloheximide (50 mg/L). Resuspended filtrates were also plated onto 10% tryptic soy agar (TSA) plus cycloheximide (50 mg/L) at 25X, 5X, and 0.5X concentrations to obtain counts of culturable bacteria on TSA (Hanlon et al., 2017). Colonies were considered culturable if they showed visible growth on TSA after 4-6 days at 22°C. Following incubation, colony forming units (CFUs) were recorded from each plate (entire plates were counted for KBC, and 1/2 of each plate was counted for TSA), and the plates were held at 4°C for ice nucleation assays (Pietsch et al., 2017). The mean colony count for KBC plates at 25X concentration was 23 CFUs per plate, providing more than the minimum 10 colonies needed to screen 30 from each location from three plate replicates. This corresponded to 5 mL of lake sample, and a mean of 4.6 CFU/mL. For TSA plates, the mean colony count at 5X concentration was 290 CFUs per plate. This corresponded to 1 mL of lake sample, and a mean of 290

CFU/mL.

3.3.5 Ice-nucleation assays

For ice nucleation assays, ten colonies were taken from three replicates of KBC plates, for a total of 30 colonies from each sampling location. A total of 720 colonies was selected at random (180 from each of the four missions). Each colony was picked with a sterile toothpick and transferred to 140 μL of water. Two droplets of 12 μL of each sample were pipetted onto floating boats made of Parafilm M placed on top of a cooling bath (Lauda Alpha RA 12, LAUDA-Brinkmann, LP, Delran, NJ, 08075) (Hanlon et al., 2017). Droplets of sterile water were used as negative controls. Samples were loaded onto the floating boats at -5°C, and the temperature of the bath was then lowered to -12°C in one degree increments. Freezing temperatures were recorded for all of the frozen droplets. Microbes from droplets freezing at temperatures warmer than -10°C were considered to be ice nucleation active (designated as ice+), and were identified using portions of 16S rDNA sequences as described by Pietsch et al. (2017).

3.3.6 Statistical analyses

Statistical analyses were conducted using R version 3.4.0. A hierarchical model and linear regression model were used to examine differences among culturable bacteria collected at 5 and 50 cm at three locations over three days. Four collection missions where conducted with one mission per day on days one and two, and two missions on day three. Statistical comparisons were made for missions one, two, and three (except when discussed otherwise). A Shapiro-Wilk normality test was used to verify data were approximately normally distributed and graphically checked using density plots and histograms. A 95% confidence interval was

used for significant differences ($P < 0.05$).

3.4 Results

3.4.1 Missions

We conducted a total of twelve sampling missions (Table 3.1) with an automated water sampler onboard a USV system. All missions were conducted from a pontoon boat (the mothership) anchored in place along the shore of the cove at the center of the sampling operations. Three sampling missions were completed in one continuous cycle each day for three days with an additional cycle being added on the third and last day (Table 3.1). During each sampling mission, the USV was controlled by remote control (RC), by the pilot in command (PIC, Schmale). The sampler was operated by a wireless link from a ground control station by a sensor operator (SO, Powers). Weather was clear with low to moderate winds and an average temperature of 11.7°C (Mission 1), 11.9°C (Mission 2), 12.2°C (Mission 3), and 17.9°C (Mission 4) during time of operation for each sampling day respectively.

Table 3.1: Mean concentrations of bacteria (CFU/mL) for KBC and TSA media. Data are reported for four sampling missions, over three days, at three locations at Claytor Lake, VA (L1, L2, and L3). Remote collections were performed with a water sampler onboard an unmanned surface vehicle (USV), and 500 mL of water was collected for each depth (5 and 50 cm) and location.

Sampling Mission	**Sampling Date**	**Sampling Time**	**Sampling Location**	**Sampling Depth**	**Mean CFU/mL KBC media ± SD**	**Mean CFU/mL TSA+C media ± SD**
1	10/25/16	11:00:00 AM	L1 (37.0426, -80.6185)	5cm	6.3 ± 0.55	196 ± 53.7
1	10/25/16	11:00:00 AM	L1 (37.0426, -80.6185)	50cm	5.3 ± 1.21	324 ± 22.6
2	10/25/16	11:05:00 AM	L2 (37.0418, -80.6188)	5cm	4.6 ± 0.35	336 ± 36.8
2	10/25/16	11:05:00 AM	L2 (37.0418, -80.6188)	50cm	4.8 ± 0.4	407 ± 86.3
3	10/25/16	11:10:00 AM	L3 (37.0433, -80.6201)	5cm	3.7 ± 0.35	291 ± 24
3	10/25/16	11:10:00 AM	L3 (37.0433, -80.6201)	50cm	2.0 ± 0.4	251 ± 80.6
4	10/26/16	11:00:00 AM	L1 (37.0426, -80.6185)	5cm	2.8 ± 0.23	198 ± 19.8
4	10/26/16	11:00:00 AM	L1 (37.0426, -80.6185)	50cm	2.6 ± 0.12	134 ± 5.66
5	10/26/16	11:05:00 AM	L2 (37.0418, -80.6188)	5cm	3.5 ± 0.55	196 ± 17
5	10/26/16	11:05:00 AM	L2 (37.0418, -80.6188)	50cm	2.7 ± 0.29	252 ± 79.2
6	10/26/16	11:10:00 AM	L3 (37.0433, -80.6201)	5cm	4.1 ± 0.52	148 ± 31.1
6	10/26/16	11:10:00 AM	L3 (37.0433, -80.6201)	50cm	3.7 ± 0.68	245 ± 1.41
7	10/27/16	11:00:00 AM	L1 (37.0426, -80.6185)	5cm	4.5 ± 0.64	390 ± 73.5
7	10/27/16	11:00:00 AM	L1 (37.0426, -80.6185)	50cm	8.1 ± 0.84	373 ± 32.5
8	10/27/16	11:05:00 AM	L2 (37.0418, -80.6188)	5cm	5.0 ± 0.2	342 ± 5.66
8	10/27/16	11:05:00 AM	L2 (37.0418, -80.6188)	50cm	5.0 ± 0.64	321 ± 157
9	10/27/16	11:10:00 AM	L3 (37.0433, -80.6201)	5cm	3.8 ± 0.53	363 ± 46.7
9	10/27/16	11:10:00 AM	L3 (37.0433, -80.6201)	50cm	3.9 ± 0.64	340 ± 19.8
10	10/27/16	01:00:00 PM	L1 (37.0426, -80.6185)	5cm	7.3 ± 1.01	311 ± 123
10	10/27/16	01:00:00 PM	L1 (37.0426, -80.6185)	50cm	5.8 ± 1.45	256 ± 127
11	10/27/16	01:05:00 PM	L2 (37.0418, -80.6188)	5cm	6.4 ± 0.35	384 ± 33.9
11	10/27/16	01:05:00 PM	L2 (37.0418, -80.6188)	50cm	7.2 ± 0.4	321 ± 35.4
12	10/27/16	01:10:00 PM	L3 (37.0433, -80.6201)	5cm	2.6 ± 1.14	227 ± 24
12	10/27/16	01:10:00 PM	L3 (37.0433, -80.6201)	50cm	5.4 ± 0.9	358 ± 19.8

3.4.2 Concentrations of bacteria on KBC and TSA

Concentrations (CFU/mL) of bacteria in water sampled from Claytor Lake were calculated using colony counts from growth on KBC and TSA media (Table 1). Concentrations ranged from 126 CFU/mL to 468 CFU/mL for microbes cultured on TSA, and from 2 CFU/mL to 46 CFU/mL for microbes cultured on KBC (Table 3.1, Figure 3.4). There was a significant difference in concentrations on KBC across three sampling locations in the lake (P = 0.027), suggesting an uneven distribution of Pseudomonas across the locations sampled. There was also a significant difference in concentrations on TSA across the three sampling days (P = 0.038), demonstrating daily fluctuations in concentrations of culturable bacteria. There was no significant difference in concentrations on TSA (P = 0.707) and KBC (P = 0.641) across the two depths sampled, suggesting microorganisms were well-mixed between 5 and 50 cm below the surface of the water.

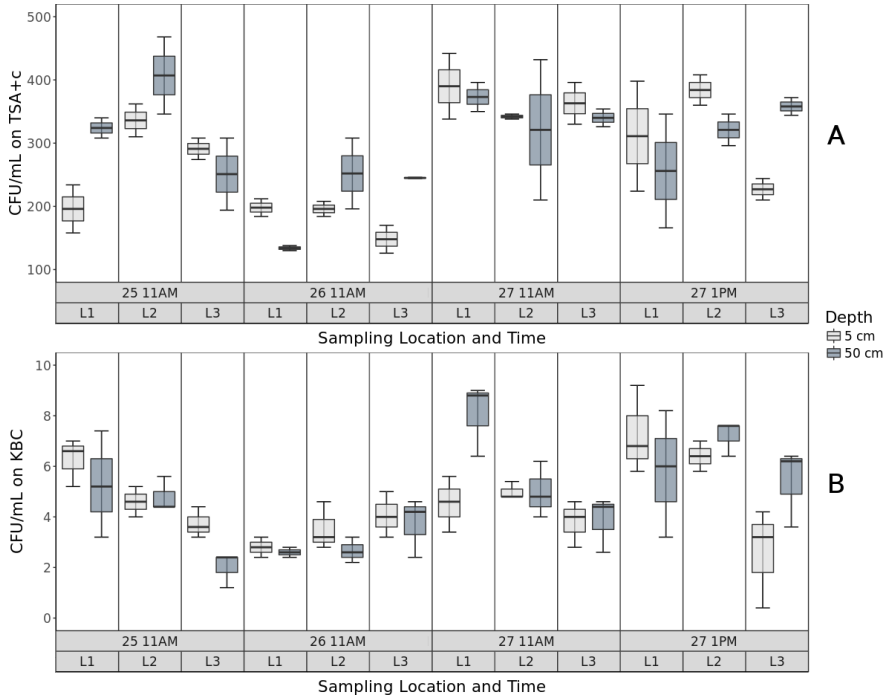

Figure 3.4: Concentrations of bacteria (CFU/mL) for TSA (A) and KBC (B) media at two depths of 5 and 50 cm at the three locations L1, L2, and L3.

3.4.3 Ice nucleation assays

720 colonies (180 colonies from each of the four missions) were tested for ice nucleation activity using a droplet freezing assay from -5°C to -12°C. Of these, seven of the colonies were ice+ at temperatures > -10°C (three ice+ from mission 1, one ice+ from mission 2, two ice+ from mission 3, and one ice+ from mission 4). Of the seven that were ice+, two were identified as Pseudomonas and one as Xanthomonas; genera that have been previously described as containing species of biological ice nucleators (Hanlon et al., 2017).

3.5 Discussion

New technologies are needed to collect and characterize the distribution of microorganisms in natural and managed aquatic environments. We developed and implemented a remote-operated water sampler onboard an unmanned surface vehicle (USV) to collect samples at multiple depths and locations. Traditional water sampling has used human-powered vehicles such as kayaks (Pietsch et al., 2017) and motorized boats (Stangl, 2001), but these missions are limited by direct human operation and line-of-sight operations. USVs have the potential to sample in remote areas, operate beyond the line-of-site, and collect samples without any human intervention. Such operations are needed in aquatic environments to increase our understanding of changes in ecosystems and improve the accuracy of our long-term predictions.

The concentration of bacteria on both media types did not vary significantly between 5 and 50 cm, when controlling for sampling location. Thus, the bacteria appeared to be well-mixed between these two sampling depths. Pietsch et al. (2017) sampled water at the surface down to about 10 m, and observed no significant change in bacteria concentration with change

in depth. Future work with the USV could probe deeper depths in the lake, to get a more accurate picture of the profile of microbes along the water column. It is possible that the difference in sampling depth (45 cm) was too small to reveal any real changes in bacterial concentrations. The maximum horizontal distance covered in this study was about 300 m in a small cove which could also be a factor. Other environmental factors, such as seasonal temperature variation and pH, are additional factors that could have an impact on bacterial distributions (Lindström et al., 2005). Such seasonal and spatial changes are known to affect lake water chemistry, which in turn impacts microbial composition in lakes (Parker et al., 2016). We speculate that samples collected at different depths could indeed show differences in concentrations of bacteria during specific times of the year (i.e., during lake turnover) (Wilhelm et al., 2014).

There was a significant difference in concentrations on KBC across three sampling locations in the lake ($P = 0.027$), suggesting an uneven distribution of Pseudomonas across the locations sampled. KBC media is selective for bacteria in the genus Pseudomonas. Bacteria in this genus are rod shaped, Gram-negative, and flagellated. The flagella enable Pseudomonas syringae to have mobility. This mobility has been shown to be beneficial to the bacteria (Lauffenburger, 1991), and is effected by temperature (Hockett et al., 2013). The difference in concentrations across locations may be related to this mobility, at least in part. The lack of significant change of concentration with location for the TSA media, could also be connected to this mobility (or lack thereof) for many bacteria. TSA is a general media type that is not selective for any particular bacteria, but is selective against fungal growth. Therefore, growth on this media includes both motile and non-motile bacteria. The difference in concentrations for the two locations (L1 and L2) may be related to geography; L1 was in a bend in the cove, offset slightly from the flow of the feeding creek from the south, and L3 was near the mouth of the cove opening up to the larger lake body (Figure 3.1). L1 may be an area of

high sedimentation caused by the redirection of water flow from the cove into the lake due to this bend. Claytor Lake is a reservoir and has been reported to have a silt problem in the past (Simmons, 2004). The cove has a narrow channelized basin impacting the trophic classification of the location towards eutrophic (Kimmel and Groeger, 1984). Sediment, which can be high in organic content, is a point source for bacteria including pathogenic strains (Kim et al., 2010). For example, concentrations of fecal coliforms were orders of magnitude higher in sediments from an agricultural stream compared to the overlying water column (Davies-Colley et al., 2004). The disturbance and re-suspension of this sediment can lead to large releases of microorganisms (Cinotto, 2005), and should be considered in the design of future sampling campaigns.

There was no significant difference in the concentration of microbes across all days for KBC media. However, there was a significant difference in the concentration of microbes from day one to day three ($P = 0.038$) for TSA media when data from the second sampling mission on day three (final day) are not included in the statistical analysis. Previous studies have reported highly variable bacteria concentrations from day to day and location to location in the same day for Claytor Lake (Pietsch et al., 2017). The undisturbed nature of the cove (limited human traffic with power boats and decreased wind interaction with the water surface due to tree cover) coupled with unique trophic characteristics, may contribute to the coves decreased day to day variation in concentrations of bacteria (Pietsch et al., 2017). Additional experiments including additional coves, depths, and seasons are needed to monitor any additional trends in microbial concentrations and potential feedback cycles.

About 1 percent (7/720) of the colonies from KBC media recovered across all four sampling missions were ice nucleation active (ice+) at temperatures warmer than -10°C. Similar ratios of ice+ Pseudomonas and Xanthomonas were found in in simulated rain samples collected from a bridge 55 m above ground level (Hanlon et al., 2017) and from real rain events at

multiple locations in Blacksburg, Virginia (Failor et al., 2017). Pietsch et al. (2017) found 6.9 % of ice+ strains in the main water body of Claytor Lake across multiple seasons. This greater percentage of ice+ bacteria as compared to our study could be related to the open waters having exposure to greater wind/surface interactions and could suggest that larger open bodies of freshwater are preferential for some ice+ bacteria. There is an important feedback cycle with microorganisms and weather as they transport from aquatic environments into the atmosphere and back down to the ground (Morris et al., 2013). These microorganisms are not only passengers along for a ride in the water cycle but may also serve as instigators for precipitation, a vital component of the water cycle. Some of these microorganisms pose health and economic risk while some serve important beneficial roles effecting the food web and climate such as Pseudomonas syringae which is both a plant pathogen and an ice nucleator that contributes to precipitation events across the globe (Morris et al., 2014). Understanding this complex interaction with aquatic environments and their inhabitants creates a rich field of study well suited to unmanned systems.

3.6 Conclusions

A remote-operated water-sampling system was used onboard a USV to collect and characterize microbes in a freshwater lake in Virginia, USA. There was an uneven distribution of Pseudomonas across the locations sampled. There was no significant difference in concentrations of microbes across the two depths sampled, suggesting microorganisms were well-mixed between 5 and 50 cm below the surface of the water. About 1 percent (7/720) of the colonies recovered across all four sampling missions were ice nucleation active (ice+) at temperatures warmer than -10°C. Our work extends traditional manned observations of aquatic environments to unmanned systems, and highlights the potential for USVs to understand the

distribution and diversity of microbes within and above freshwater aquatic environments.

Tracking microorganisms such as Pseudomonas syringae throughout the entire water cycle could help to reveal a fundamental component of the water cycle and its role in both local and global weather and other important environmental processes (Morris et al., 2008). Such a study would require unmanned systems working together to sample in and above the water. Research conducted by autonomous coordinated systems (Kolling et al., 2016; Vardy, 2016) could reveal a wealth of information on transport patterns of microorganisms and associated environmental impacts. These studies could be comprised of surface, aerial and ground vehicles working as a heterogeneous swarm (Szwaykowska et al., 2015) to sample and characterize the environment with sophisticated meteorological sensors (e.g., windspeed, air and water temperature, solar radiation, etc.) and biological sensors (e.g., impingers (Lin et al., 1999) and optical particulate counters (Lee et al., 2006)). Such studies could also include laboratory measurements of CFU (Pietsch et al., 2017), and flow cytometry measurements for to characterize cell sizes and concentrations (Buzatu et al., 2014). Future work using these highly adaptive autonomous systems over diurnal and longer seasonal cycles could capture an unprecedented in depth and detailed picture of the role of these microorganisms in a range of environmental systems.

3.7 Acknowledgements

This research was supported in part by the National Science Foundation (NSF) under Grant Numbers DEB-1241068 (Dimensions: Collaborative Research: Research on Airborne Ice-Nucleating Species (RAINS)), DGE-0966125 (IGERT: MultiScale Transport in Environmental and Physiological Systems (MultiSTEPS)), and IIS-1637915 (NRI: Coordinated Detection and Tracking of Hazardous Agents with Aerial and Aquatic Robots to Inform Emergency

Responders). Any opinions, findings, and conclusions or recommendations expressed in this material are those of the authors and do not necessarily reflect the views of the NSF.

Chapter 4. Coordinated sampling of biological aerosols over freshwater and saltwater environments using an unmanned surface vehicle (USV) and a small unmanned aircraft system (sUAS)

Craig W. Powers, Regina Hanlon, David G. Schmale III*

Status: Draft

4.1 Abstract

Biological aerosols are ubiquitous in terrestrial and aquatic environments and may influence cloud formation and precipitation processes. Little is known about the aerosolization and transport of biological aerosols from aquatic environments. We designed and deployed a bioaerosol-sampling system onboard an unmanned surface vehicle (USV, a remotely-operated boat) to collect microbes and monitor particle sizes in the atmosphere above a salt pond in Falmouth, Massachusetts, USA and a freshwater lake in Dublin, Virginia, USA. The bioaerosol-sampling system included a series of 3D-printed impingers, two different optical particle counters, and a weather station. A small unmanned aerial system (sUAS, a remotely-operated airplane) was used in a coordinated effort with the USV to collect microorganisms

on agar media 50 m above the surface of the water. Samples from the USV and UAS were cultured on selective media to estimate concentrations of culturable bacteria. Samples from the sUAS ranged from 29 to 72 CFU (10 minute sampling) at heights of 50 m per flight, and samples from the USV ranged from 0 to over 4,000 CFU/mL (30 minute sampling at 1.8 and 2.2 Lpm respective of the two media types) near the water surface. Particle concentrations recorded onboard the USV ranged from 0 to 288 $\mu g/m^3$ for PM1, 1 to 290 $\mu g/m^3$ for PM2.5, and from 1 to 290 $\mu g/m^3$ for PM10. A general trend of increasing concentration with increase in particle size was recorded by each sensor. Future work aims to understand the distribution of biological aerosols above aquatic environments and their potential association with cloud formation and precipitation processes.

4.2 Introduction

Aerosols are microscopic particulate matter (PM) that become airborne at the planetary surface, usually from turbulent air, and remain suspended in the atmosphere (Millner, 2009; Vincent, 2007). These aerosols can be from anthropogenic or natural sources, i.e. dust and smoke, or secondary particulates (SOx, NOx, and VOCs) that are formed in the atmosphere from chemical reactions. (Colbeck et al., 2014). Transport of some aerosols is known to occur over long distances in the atmosphere; African dust has been observed to be transported westward over the Atlantic and to North America and to Europe over the Mediterranean (Kersey, 2000). Aerosols can have harmful health effects on humans, and can serve as a central component to environmental problems, for example, photochemical smog, poor air quality, and global warming (Colbeck et al., 2014). Aerosols can also be biological in nature, and are often referred to as biological aerosols (bioaerosols).

Bioaerosols are generally small, from 0.02 μm to 50 μm (bacteria, fungal spores, pollen,

and algae), and can be living or dead cells (Cox and Wathes, 1995). Microorganisms that become bioaerosols can be harmless viruses, bacteria or fungi that do not directly impact human health, but some are highly infectious, produce hazardous byproducts or can trigger an immunological response in humans (Cherrie et al., 2011). Some of these bioaerosols, such as *Pseudomonas syringae*, are known plant pathogens (Ichinose et al., 2013) and have been suggested as contributors to cloud ice nucleation and precipitation events (Hallar et al., 2012; Morris et al., 2008). This is possible due to the expression of an ice nucleation active (INA) protein allowing *P. syringae* to initiate the freezing of water at temperatures at approximately -2 deg C, which is much warmer than normally required for water that is free from particulates (Cohen et al., 2001; Maki et al., 1974; Morris et al., 2004). *P. syringae* is considered to be one of the most effective ice nucleators, biotic or abiotic, and therefore, one of the largest causes of surface frost damage in plants (Hirano, 1995; Maki et al., 1974). Little is known about the sources, aerosolization and transport of *P. syringae* and other biological aerosols and their interactions with the environment (Fröhlich-Nowoisky et al., 2016). New scientific tools are needed to study these bioaersols and their global impact.

New and improved environmental sensors are enabling researchers to study biological aerosols in natural environments with an unprecedented level of sophistication and detail. Many of these sensors can be mounted on unmanned systems, such as unmanned aircraft systems (UASs) and unmanned surface vehicles (USVs). These unmanned systems can help gather data in a safe and cost effective manner that, in some cases, would otherwise be impossible, for human based endeavors. Smaller unmanned systems such as USVs and UASs, have become useful remote sampling platforms and when used in coordinated sampling efforts, can begin to accomplish sampling goals needed to study aerosols on larger spatial scales (Bamberger Jr et al., 2006; Duarte et al., 2016).

The ultimate goal of this research was to develop a method to monitor biological aerosols

above saltwater and freshwater aquatic environments using environmental sensors onboard a USV and sUAS. The specific objectives were to (1) design an automated sampler to collect microbes and monitor particle sizes and (2) use a USV and sUAS in a coordinated study to monitor the distribution of bioaerosols above a saltwater and a freshwater aquatic environment.

4.3 Materials and Methods

4.3.1 Study site

Field experiments were conducted at a saltwater pond, the Great Pond, Falmouth, MA, USA(41.5580N 70.5841W), and a freshwater lake, Claytor Lake, Dublin, VA, USA (37.0530N 80.6208W). The Great Pond is a large salt water pond that is connected to the ocean. Claytor Lake is a fresh water reservoir fed by the New River.

4.3.2 Unmanned surface vehicle

An electric unmanned surface vehicle from Clearpath Robotics Kingfisher USV (Clearpath Robotics, Kitchener, Ontario, Canada) 4.3 served as the base sampling platform for collecting and measuring bioaerosols in both aquatic environments. This Kingfisher USV has a catamaran hull and was approximately 30 kg in weight with payload, with dimensions 1.35 m $\times$ 0.98 m $\times$ 1.2 m (L $\times$ W $\times$ H), as equipped for use in this study. The Kingfisher was operated via remote control. Batteries provided about 3 hours of runtime and could be exchanged when needed. The propulsion system was a differential thrust system driven by two impellers inside each of the two hulls giving a maximum speed of 1.7 ms, allowing for precise movements in shallow waters with little disturbance to the surrounding aquatic

environment that could affect sampling. Six 30-minute USV sampling missions were conducted at Great Pond, and six 30-minute USV sampling missions were conducted at Claytor Lake 4.1. For the Great Pond experiments, sampling missions were conducted from about 10:00 AM to 15:00 PM EST on August 20th 2017 (Table 4.1). For the Claytor Lake experiments, sampling missions occurred from about 11:30 AM to 15:30 PM EST on October 3rd 2017 (Table 4.1). Each sampling mission consisted of loading six impingers with fresh sterile water. The UAV then transitioned to the sampling location using visual markers such as buoys for guidance. Once in place the USV was holding position, using thrusters only to stay pointed into the wind and on location. The sampling platform was extended to the vertical position. Data collection from particle and meteorological sensors was started. Vacuum pumps for the appropriate impingers were turned on. Sampling was continued for 30 minutes. At the conclusion of the 30-minute sampling duration, the vacuum pumps were turned off and recording of particle and meteorological data was completed. The sampler platform was returned to the stowed configuration and the USV transitioned back to the shore. Impingers were removed and the 50mL conical tubes were be unscrewed from the impinger body and capped with sterile lids. The impinged samples were then placed on ice and transported to the laboratory for processing after the conclusion of all sampling missions for the day.

4.3.3 Small Unmanned Aircraft System (sUAS)

A small unmanned aircraft system (sUAS) was used collect microorganisms in the lower atmosphere. Flights were coordinated within the USV sampling periods such that both vehicles were sampling simultaneously. The sUAS flew an orbital (circular) pattern with a target altitude of 50 m AGL, with the USV at the approximate center of the orbit. The sUAS platform was an electric fixed-wing pusher platform (the Clouds Fly AXN) with a remote-

controlled microbe-sampling device. The sUAS was equipped with the Hitec Sensor Station (HTS-SS) including pitot airspeed (HTS-AS) and GPS (HTS-GPS) sensors. The microbe-sampling device consisted of a single 60 mm vertically-mounted petri plate containing agar media. This is a modification of the design used by (Schmale et al., 2008, 2012) and (Techy et al., 2010). The sampling device was closed during takeoff and landing, and was opened by remote control from the ground once the sUAS was at the target sampling altitude and airspeed. The device remained open for the duration of the 10-minute sampling interval. Immediately following sample collection, the exposed plate containing the agar media was removed from the sampling device and stored in a small plastic container for transport to the laboratory. Flights were conducted by a Federal Aviation Administration (FAA)-certified pilot (Schmale) under Remote Pilot Certificate Number 4038906. Flights over Claytor Lake, VA were conducted under State Parks Special Use Permit Number 4-012-017 issued by Chris Doss, Park Manager.

4.3.4 Development of an automated atmospheric sampler and sensor integration on a USV

A bioaerosol-sampling system was integrated into the USV to sample at at different heights above and below the water. Four optical particle counters from two different manufactures, the SDS021 (Nova Fitness Co., Ltd., Jinan,Shandong Province) and the PMS7003 (Plantower, shunyi District,Beijing), were used (Figure 2). One of each type of sensor was placed at 0.1 m and 1.1 m above the water, so that at each height, there were two different types of sensors (Figure 4.1). The SDS021 reported PM2.5 and PM10 concentrations while the PMS7003 reported PM1, PM2.5 and PM10 concentrations. These sensors collected measurements at a sampling rate of about 1Hz. In addition to the PM counters, a custom impinger was designed and printed from high-density polyethylene (which allowed the impinger to be

autoclaved). The impinger was designed to be screwed directly onto a 50 mL sterile conical

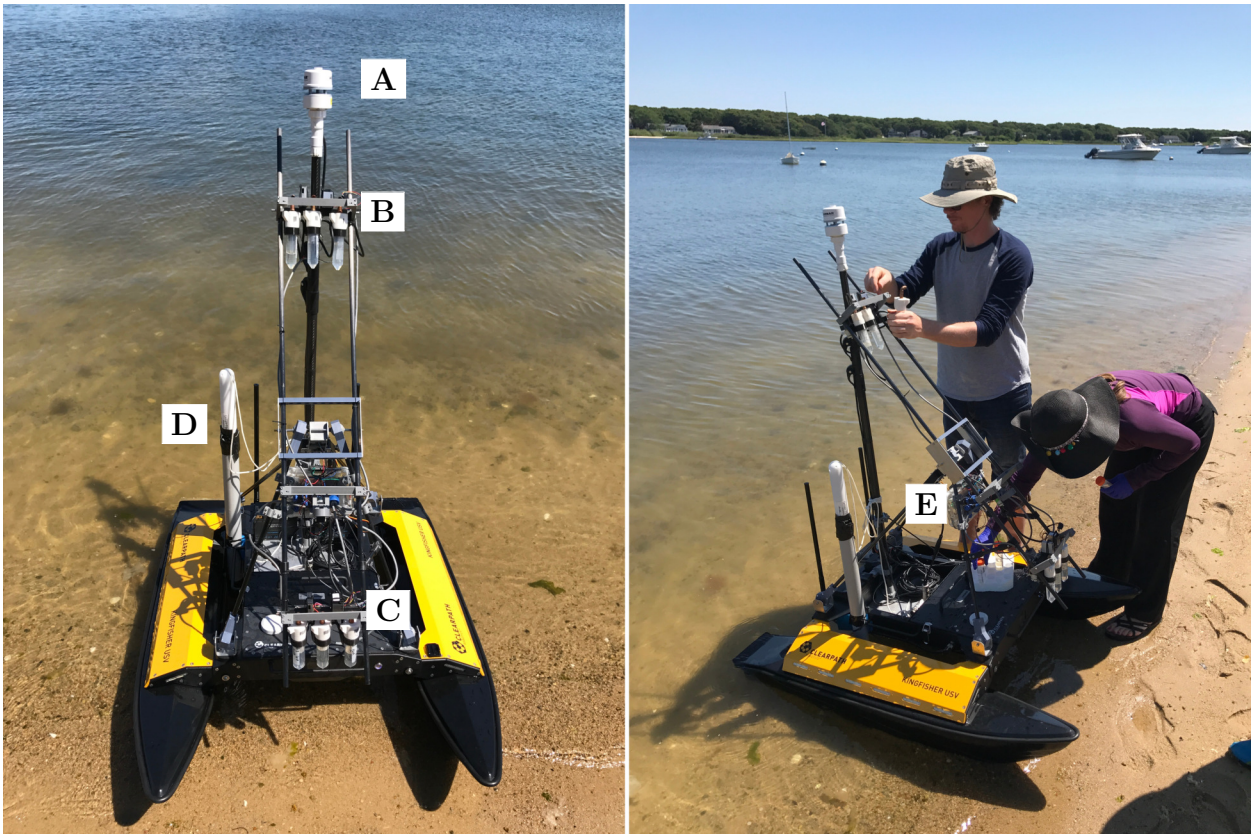

Figure 4.1: Sampler deployed on USV in Boston MA. An Airmar 200WX sensor (A) was used to capture meteorological data. A set of three impingers and two particle counters were used at 1.1 m (B) and 0.1 m (C) when deployed. A Turner turbidity sensor was also used. The sampler is seen in the stowed configuration (E) and is extended to a vertical position when sampling.

centrifuge tube (Corning CLS430828 SIGMA). The impinger was also designed around disposable Pasteur pipettes (Corning CLS7095D5X SIGMA) as the down tube that air would travel through into the impinger liquid. A 1 cm diameter copper plumbing elbow served as the air inlet to the impinger. The choice of copper and glass surfaces minimized adhesion of particles to the impinger before being deposited into the fluid. The impinger design was guided in part by impinger design testing made by Lin et al. (1997) to ensure the highest possible collection efficiency. Three impingers at each height (0.1 m and 1.1 m) were used

along side the paired PM counters so that particulates could be collected in liquid media by impingers while PM counters counted particle concentrations for the same spatial location above the water surface 4.3. Each impinger was connected to a pump modified to operate as a vacuum pump (ZT370-01, Dongguan Zhentian precision electronic co., LTD, Dongguan city, Guangdong province, China.) pulling from 1.6 to 2.4 Lpm of air to the impinger nozzle down the pipette tube where it then traveled through 35 ml of liquid media in the conical tube. Three of these impingers where used in two groups that included two PM counters (one of each manufacturer) with one sensor group at 0.1 m above the water surface and the second sensor group at 1.1 m above the water surface. These sensor groups were mounted on a two vertical carbon fiber tubes attached to a carbon fiber tubing base attached to the USV (Figure 4.1). The carbon fiber base allowed the vertical sensor assembly to be rotated about 45 degrees aft via a stepper motor screw assembly for safe transport between sampling missions. The sensors, vacuum pumps, and stepper motor where connected to a 3teensy 3.6 ARM based microcontroller (PJRC.COM, LLC., Sherwood, Oregon, USA) that controlled all sensor operations. An Airmar 200WX marine weather station was integrated into the USV to capture environmental data including wind speed, wind direction, and temperature. All sensor data was transmitted to the USV computer via serial communications for recording. Sensor actuation and data collection were controlled through the USV computer by a command computer on shore over 2.4GHz wifi hotspot link.

4.3.5 Collection and culturing of microorganisms from sUAS

Agar collection plates from the sUAS sampling missions contained R2A or OceanMod media. R2A was fresh water bacteria selective media and OceanMod was saltwater selective media. Plates were incubated for 3-4 days at room temperature, and colony forming units (CFUs) were counted and the plates were photographed. A subset of the colonies on each plate were

picked with sterile toothpicks and inoculated into 140 μL of H_2O for ice nucleation assays and subsequent storage at -80 C in 20% glycerol.

4.3.6 Statistical analyses

Statistical analyses were conducted using R version 3.4.2. A linear regression model was used to examine differences among culturable bacteria collected during twelve sampling missions over two days with meteorological and PM concentration data. A circular linear regression model was used to compare wind direction with PM concentration data. A 95% confidence interval was used for significant differences ($P < 0.05$).

4.4 Results

4.4.1 USV, Great Pond, Falmouth, MA

Six USV missions were conducted on 20 August 2017. The concentration of culturable bacteria ranged from 0 to 2990 CFUs/mL on R2A and ranged from 0 to 54 CFUs/mL on OceanMod, respectively. Particulate matter concentrations ranged from 2 to 8 $\mu g/m^3$ for PM1, 3 to 24.1 $\mu g/m^3$ for PM2.5 and 3 to 25.4 for $\mu g/m^3$ (Table 4.1). Figure 4.2 gives PM concentrations for the six missions with outliers removed.

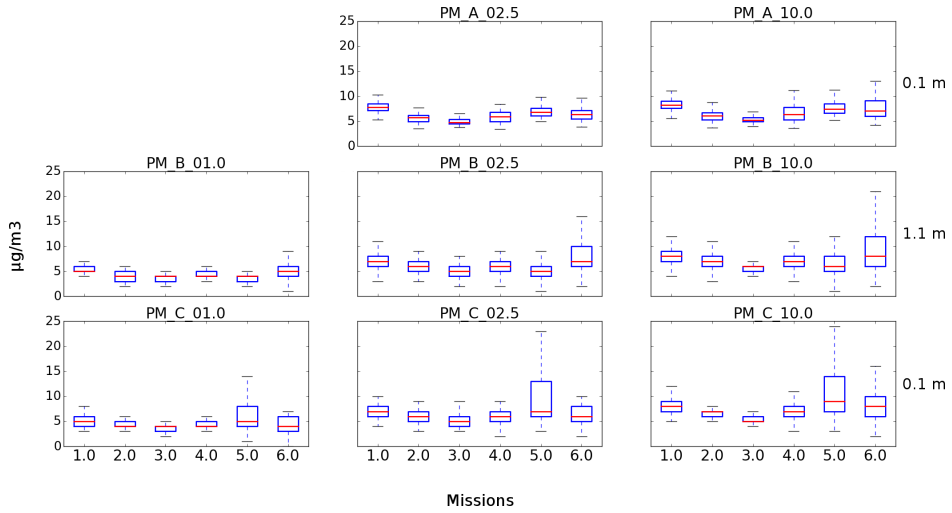

Figure 4.2: Particle count concentrations from the Great Pond, Falmouth, MA. Three of the four integrated particle sensors where operational for the six missions. The top row represents the SDS021 sensor at 0.1 m for PM2.5 and PM10. The middle row represents the PM7003 sensor at 1.1 m for PM1, PM2.5 and PM10. The bottom row represents the PM7003 sensor at 0.1 m for PM1, PM2.5 and PM10.

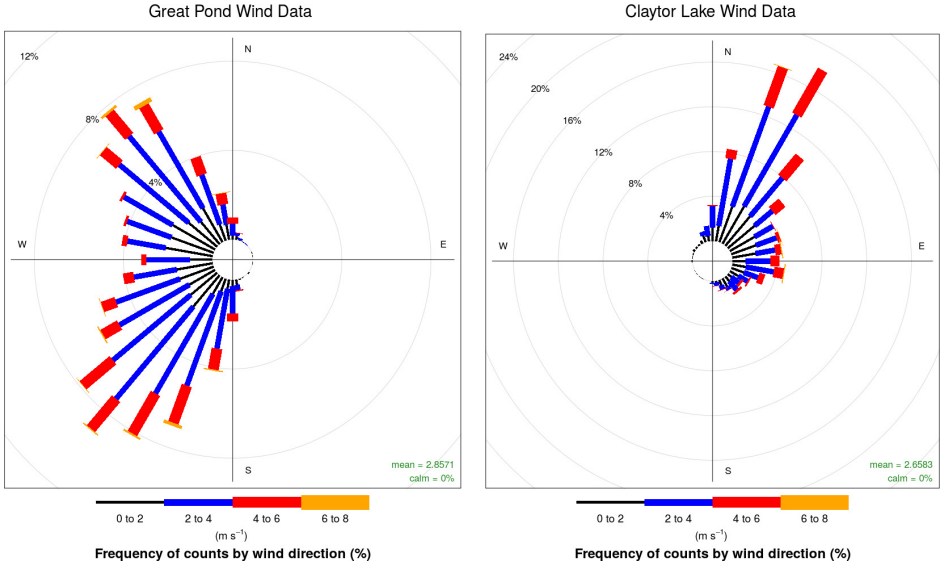

Figure 4.3: Wind plots for the Great Pond MA and Claytor Lake VA. Colors represent the speed of wind with legth of bars representing the percentage of time at the given windspeed.

4.4.2 USV, Claytor Lake, Dublin, VA

Six USV missions were conducted on 3 October 2017. The concentration of culturable bacteria ranged from 322 to 4005 CFUs/mL on R2A and OceanMod plates had no growth. Particulate matter concentrations ranged from 0 to 288 μg/m^3 for PM1, from 2.5 to 18 μg/m^3 for PM2.5 and from 2.6 to 19 μg/m^3 for PM10 (Table 4.1). Figure 4.4 gives PM concentrations for the six missions with outliers removed.

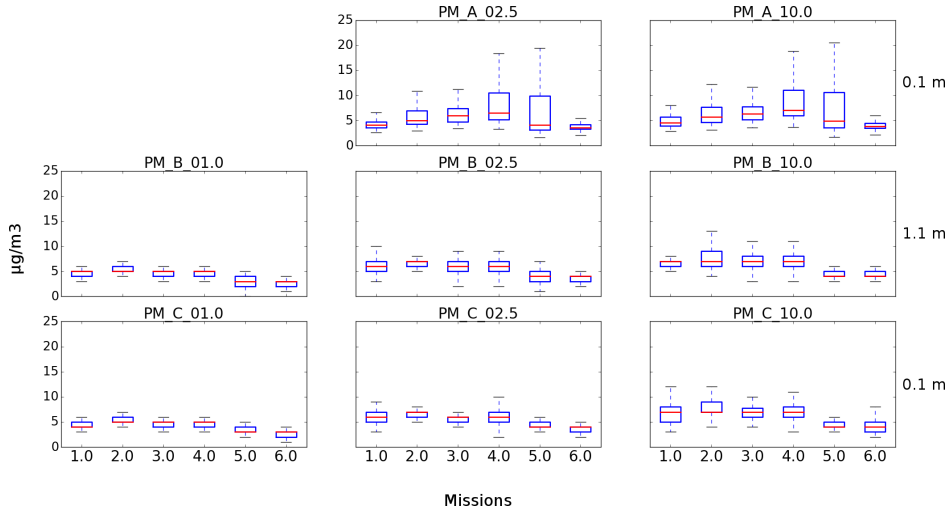

Figure 4.4: Particle count concentrations from Claytor Lake, Dublin, VA. Three of the four integrated particle sensors where operational for the six missions. The top row represents the SDS021 sensor at 0.1 m for PM2.5 and PM10. The middle row represents the PM7003 sensor at 1.1 m for PM1, PM2.5 and PM10. The bottom row represents the PM7003 sensor at 0.1 m for PM1, PM2.5 and PM10.

4.4.3 Missions

Table 4.1: USV biological data for impinger sampling. Samples from 0.1 and 1.1 m where combined before plating for volumetric requirements.

Sample Number	Date	Time Start Sampling (EST)	Location (GPS)	Media	CFUs per mL	PM1 $\mu g/m^3$ Min Max	PM2.5 $\mu g/m^3$ Min - Max	Pm10 $\mu g/m^3$ Min - Max
MA_1	8/20/17	10:15 AM	41.557817, -70.582646	MOB	0	2 - 8	3 - 24.1	3 - 25.4
MA_1	8/20/17	10:15 AM	41.557817, -70.582647	R2A	2			
MA_2	8/20/17	11:09 AM	41.557817, -70.582648	MOB	0	3 - 5	4.9 - 7	5.2 - 8
MA_2	8/20/17	11:09 AM	41.557817, -70.582649	R2A	0			
MA_3	8/20/17	12:28 PM	41.557817, -70.582650	MOB	0	3 - 4	3 - 6	3 - 7
MA_3	8/20/17	12:28 PM	41.557817, -70.582651	R2A	0			
MA_4	8/20/17	12:49 PM	41.557817, -70.582652	MOB	54	4 - 6	4.6 - 7	4.9 - 8
MA_4	8/20/17	12:49 PM	41.557817, -70.582653	R2A	2990			
MA_5	8/20/17	01:38 PM	41.557817, -70.582654	MOB	5	2 - 5	3 - 7	3 - 10
MA_5	8/20/17	01:38 PM	41.557817, -70.582655	R2A	0			
MA_6	8/20/17	02:25 PM	41.557817, -70.582656	MOB	0	3 - 5	4 - 9	4 - 10
MA_6	8/20/17	02:25 PM	41.557817, -70.582657	R2A	14			
CL_1	10/03/17	11:26 AM	37.052780, -80.619517	MOB	0	4 - 6	4.1 - 7	4.9 - 7
CL_1	10/03/17	11:26 AM	37.052780, -80.619518	R2A	4005			
CL_2	10/03/17	12:12 PM	37.052780, -80.619519	MOB	0	5 - 67	4 - 6	6 - 7
CL_2	10/03/17	12:12 PM	37.052780, -80.619520	R2A	1257			
CL_3	10/03/17	01:00 PM	37.052780, -80.619521	MOB	0	1 - 70	4.9 - 6.3	5.4 - 7
CL_3	10/03/17	01:00 PM	37.052780, -80.619522	R2A	1615			
CL_4	10/03/17	01:58 PM	37.052780, -80.619523	MOB	0	1 - 52	6 - 18	6 - 19
CL_4	10/03/17	01:58 PM	37.052780, -80.619524	R2A	752			
CL_5	10/03/17	02:52 PM	37.052780, -80.619525	MOB	0	0 - 288	3 - 4	3 - 4
CL_5	10/03/17	02:52 PM	37.052780, -80.619526	R2A	872			
CL_6	10/03/17	03:35 PM	37.052780, -80.619527	MOB	0	0 - 29	2.5 - 4	2.6 - 4.4
CL_6	10/03/17	03:35 PM	37.052780, -80.619528	R2A	322			

4.4.4 sUAS

Four sUAS missions were conducted on 20 August 2017 at the Great Pond, Falmouth, MA, and four sUAS missions were conducted on 3 October 2017 at Claytor Lake, Dublin, VA. For the sUAS missions in MA, CFUs ranged from 40 to 44 for R2A and from 29 to 35 for OceanMod, respectively. For the sUAS missions in VA, CFUs ranged from 55 to 59 for R2A and from 60 to 72 for OceanMod, respectively (Table 4.2).

Table 4.2: UAS biological data for plate deposition sampling

Flight Number	Date	Time Plate Open (EST)	Location (GPS)	Media	CFU per plate	Colonies Screened	Ice+	% Ice+
FSalt1	8/20/2017	11:16 AM	41.557817, -70.582646	OceanMod	29	12	0	0
FSalt2	8/20/2017	12:05 PM	41.557817, -70.582646	R2A	40	18	0	0
FSalt3	8/20/2017	12:52 PM	41.557817, -70.582646	OceanMod	35	18	0	0
FSalt4	8/20/2017	1:43 PM	41.557817, -70.582646	R2A	44	16	0	0
FFresh1	10/3/2017	11:44 AM	37.052780, -80.619517	OceanMod	60	13	0	0
FFresh2	10/3/2017	12:24 PM	37.052780, -80.619517	R2A	59	24	0	0
FFresh3	10/3/2017	2:06 PM	37.052780, -80.619517	OceanMod	72	24	1	4
FFresh4	10/3/2017	2:59 PM	37.052780, -80.619517	R2A	55	25	4	16

Results of statistical analyses

The SDS0021 sensor at 0.1 m showed a significant correlation with wind speed reported by the USV mounted meteorological sensor at Claytor Lake, VA for PM2.5 (P=1.07×10^{-6}), PM2.5 and PM10 (P=7.33×10^{-7}). Correlations were also found at the Great Pond, MA for wind speed with PM2.5 (P=0.016) and PM10 (P=0.006) for the PMS7003 senor at 0.1 m and PM2.5 (P<2×10^{-16}) and PM10 (P=0.0316) for the SDS0021 sensor at 0.1 m. CFU/mL ranged from 0 to 2990 CFU/mL for the Great Pond, MA and 0 to 4005 CFU/mL for Claytor Lake.

PM sensors for Claytor Lake, VA reported similar concentrations (P values ranged from 5.24×10^{-07} to 3.86×10^{-10}) except the SDS0021 sensor at 0.1 m with both PMS7003 senors at 0.1 m and 1.1 m for PM2.5 and PM 10 (P values ranged from 0.299 to 0.551). Concentrations where on average higher at 1.1 m than 0.1 m for all sensors and all PM sizes. PM sensors for the Great Pond, MA reported similar concentrations (P values ranged from 5.47×10^{-12} to $< 2 \times 10^{-16}$). Concentrations where on average lower at 1.1 m than 0.1 m for all sensors and all PM sizes.

PM conentrations where highly correlated with wind direction for all sensors and PM sizes at Claytor Lake, VA (P= $< 2 \times 10^{-16}$) and the Great Pond, MA (P values ranged from $< 3.81 \times 10^{-06}$ to $< 2 \times 10^{-16}$).

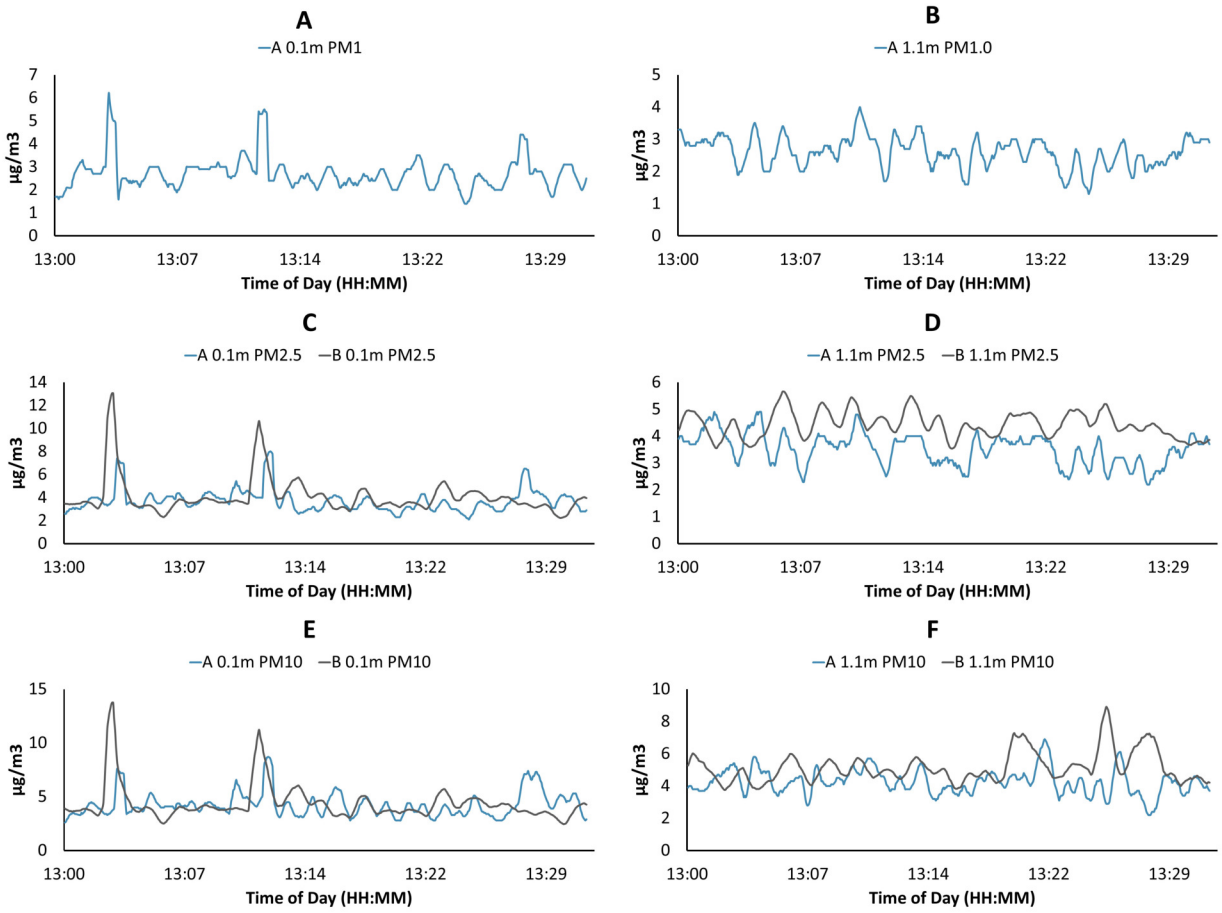

Figure 4.5: Plots of particle data from October 3^{rd} 2017 on Claytor Lake. Two model of optical particle counters PMS7003(A) and SDS021(B) where used. Only the PMS7003(A) sensor was able to resolve PM1 at 0.1m above the water surface (A) and PM1 at 1.1m (B). Both models reported PM2.5 at 0.1m (C), PM2.5 at 1.1m (D), PM10 at 0.1m (E) and PM10 at 1.1m (F). Graphs are in general accordance both in shape and averages with some minor variations.

4.5 Discussion

The sources, distribution, and transport of biological aerosols are not well understood. New information is needed regarding the impacts of biological aerosols on climate (Fröhlich-Nowoisky et al., 2016). We developed and implemented a bioaerosol-sampling system onboard a USV to collect and characterize biological aerosols at multiple heights above saltwater and freshwater environments. Several sensors were integrated into the system including a series of 3D printed impingers, four optical particle sizers, and a meteorological sensor. A sUAS was used to collect microorganisms on agar media 50 m above the surface of the water. Use of coordinated unmanned systems with atmospheric samplers and sensors, can be used to characterize the distribution and transport of microbes and aerosols above aquatic environments. CFU/mL ranged from 0 to 2990 CFU/mL for the Great Pond, MA and 0 to 4005 CFU/mL for Claytor Lake, VA, for USV impinger samples 4.2. This is an extremely wide range of CFU/mL and may point to the variability of bioaerosols, in the scope of minutes to hours, present in aquatic environments. Some microorganisms such as *Pseudomonas syringae* are ubiquitous in aquatic environments (Morris et al., 2013), and have been found to be highly variable in spatial distribution in freshwater lakes (Pietsch et al., 2017). This variability could have an impact on the large range of CFU/ml of culturable bacteria. There was no significant difference in CFU/mL for colonies collected on the USV on both R2A and MOB media for both missions (P values ranged from P=0.17 to P=0.92). The lack of correlation from PM sensors is likely due to the small sample size. It is possible that the aerosolization of culturable bacteria for the time frame and season sampled is random. More sampling is needed over longer time periods and seasons.

Wind speed varied from 1 to 9.5 knots at the Great Pond, MA and varied from 1.4 to 9.5 knots during sampling at Claytor Lake, VA (Figure 4.3). PM concentrations from the four PM sensors where in general agreement in average concentrations and concentration

variations (Figure 4.5). Particle sensors at 0.1 m showed a significant correlation with wind speed reported by the USV mounted meteorological sensor at Claytor Lake, VA and at the Great Pond, MA. The connection with higher particle concentrations with increased wind suggests vertical mixing at the MABL where the characteristic timescale for mixing of gases and aerosols is on the order of seconds (Jonsson et al., 2014). This connection is what we should expect to see and is partial validation of the sensors ability to operate effectively in this time scale at this altitude. Different levels of sensitivity or accuracy between the PMS7003 and SDS0021 sensors could explain the consistently different correlation of the sensors. The lack of correlation at the 1 micron particle size could indicate a continuous background noise of sea salt particulates being reported at the MABL (Gong et al., 1997). Sea salt aerosols are important as they play significant roles in clear sky radiative forcing and serve as a source of cloud condensation nuclei (Winter and Chỳlek, 1997; Gras and Keywood, 2017). Understanding what exactly are the components of the aerosols reported by the particle counters, sea salt or otherwise, remains a challenge and will require further testing and validation of all sensors.

Future work could probe deeper associations of connections of culturable bacteria, wind speed, and particle concentrations at the air-water interface. Such work could contribute to our understanding of the sources and transport of biotic and abiotic aerosols and their linkages to global health.

4.6 Acknowledgements

This research was supported in part by the National Science Foundation (NSF) under Grant Numbers DEB-1241068 (Dimensions: Collaborative Research: Research on Airborne Ice-Nucleating Species (RAINS)), DGE-0966125 (IGERT: MultiScale Transport in Environmental and Physiological Systems (MultiSTEPS)), AGS- 1520825 (HAZARDS SEES: Uncovering the Hidden Skeleton of Environmental Flows: Advanced Lagrangian Methods for Hazard Prediction, Mitigation, and Response), and IIS-1637915 (NRI: Coordinated Detection and Tracking of Hazardous Agents with Aerial and Aquatic Robots to Inform Emergency Responders). Any opinions, findings, and conclusions or recommendations expressed in this material are those of the authors and do not necessarily reflect the views of the NSF.

Chapter 5. Tracking of a fluorescent dye in a freshwater lake with an unmanned surface vehicle and an unmanned aircraft system

Craig W. Powers, Regina Hanlon and David G. Schmale III*

Submitted: November 2017

To: Remote Sensing

Status: In review

5.1 Abstract

Recent catastrophic events in our oceans, including the spill of toxic oil from the explosion of the Deepwater Horizon drilling rig and the rapid dispersion of radioactive particulates from the meltdown of the Fukushima Daiichi nuclear plant, underscore the need for new tools and technologies to rapidly respond to hazardous agents. Our understanding of the movement and aerosolization of hazardous agents from natural aquatic systems can be expanded upon and used in prevention and tracking. New technologies with coordinated unmanned robotic systems could lead to faster identification and mitigation of hazardous agents in lakes, rivers, and oceans. In this study, we released a fluorescent dye (fluorescein) into a freshwater

lake from an anchored floating platform. A fluorometer (fluorescence sensor) was mounted underneath an unmanned surface vehicle (USV, unmanned boat) and was used to detect and track the released dye in situ in real-time. An unmanned aircraft system (UAS) was used to visualize the dye and direct the USV to sample different areas of the dye plume. Image processing tools were used to map concentration profiles of the dye plume from aerial images acquired from the UAS, and these were associated with concentration measurements collected from the sensors onboard the USV. The results of this project have the potential to transform monitoring strategies for hazardous agents, enabling timely and accurate exposure assessment and response in affected areas. Fast response is essential in reacting to the introduction of hazardous agents, in order to quickly predict and contain their spread.

5.2 Introduction

The spread of hazardous agents such as radioactive particulates, oil, and harmful algal blooms have important economical (Fay, 2003), ecological (Anderson et al., 2005), and national security (Lien et al., 2007) consequences. There are numerous mathematical models and methods for understanding and predicting how these agents are transported and dispersed, from ground water contamination to volcanic eruptions (Csanady, 1973; Gunatilaka et al., 2012). Many of these methods are computationally costly or may not be adaptive for highly variable environments that exist in real world scenarios. Additionally, these computational approaches may not be applicable for first responder scenarios for remote locations, where there is limited information available to populate necessary model parameters. In many cases, diffusion and advection dominance is highly variable and competition between the two transport mechanisms can be complex. This occurs especially at the marine atmospheric boundary layer (MABL), where both aquatic and wind currents interact, further

complicating modeling techniques. In these situations, when a fast solution is required and the exact solution may not be important, a simpler approach is needed. Heuristic methods represent such an approach (Cook, 1983).

Oil is one hazardous agent that can have immediate and lasting impacts in marine environments for a considerable time after initial release, and in the case of salt marshes and mangrove swamps, effects can persist for decades (Kingston, 2002). Oil leakage from offshore oil and natural gas exploration can be affected by factors at the ocean bottom not encountered at the sea surface, complicating detection and tracking (Masutani and Adams, 2001). Spills from large oil tankers, though dangerous occurrences, account for only 5% of worldwide oil pollution, with 95% accounted for by illegal discharges (Galland et al., 2004). Other hazardous agents include harmful algal blooms (HABs), microscopic algae or phytoplankton that can be beneficial in nature, but also can be harmful to marine resources and human health (Lewitus et al., 2012). In some cases, surface roughness at the marine atmospheric boundary layer can make satellite measurements prone to errors (Klemas, 2011). Versatile and adaptable tracking methods are needed.

A number of tracer dyes have been used to understand the transport of hazardous agents in aquatic environments. These dyes are often fluorophores, like rhodamine and fluorescein (Vasilijevic et al., 2015; Jackson and Lageman, 2013; Li et al., 2006), and sensors known as fluorometers have been developed to detect these dyes following their release (Barczewski and Marschall, 1990; Funkhouser and Barks, 2004). These sensors have been used to test simulated fluorophore plume identification and verification algorithms in near-shore oceanic environments (Tian et al., 2013). In addition to specially developed sensors, effective lower cost methods have been used. Cameras have been used to measure the motion of fluorescent particles in surface flow studies (Tauro et al., 2012). Fluorescent dyes have been used in underwater studies to test the effectiveness of hydrocarbon detection (Vasilijevic et al., 2015).

Direct measurements of fluorescent organisms is another method of plume detection and tracking. Algae can absorb certain wavelengths of light and remit this gained energy at another wavelength (Qian et al., 2010) similar to fluorophores. Consequently, fluorometers have been developed to detect algae in situ (Mason, 1999). Fluorophores for aquatic studies are often used that absorb and emit light in wavelengths that naturally pass through water unaffected over the characteristics scale lengths from the sensor emitter to sensor receiver.

Unmanned systems have become important tools to increase our understanding of vital environmental processes. Recent advances in unmanned systems have created new possibilities for environmental sensing (Pennington et al., 2016). Low cost unmanned surface vehicles (USVs) have been developed allowing water quality testing by citizen science programs that would not be possible otherwise due to budgetary constraints (Laut et al., 2014a). Theses systems are effective outreach tools promoting environmental science to the general public (Laut et al., 2014b). Likewise, low-cost recreational unmanned aircraft systems (UASs) with gimbal mounted cameras have served as platforms for surface flow measurement mapping using natural and artificial tracers and large-scale surface velocity fields (Tauro et al., 2016; Detert and Weitbrecht, 2015). UASs have applications in hydrological studies to measure lake and river water levels to increase our understanding of hydrologic processes and reliability of hydrologic predictions (Bandini et al., 2017a,b).

There are significant knowledge gaps in the transport of hazardous agents in aquatic systems, and unmanned systems help fill this gap by incorporating measurements of fluorescence to mimic hazardous agent dispersal. The specific objectives of this work were to detect and track a released dye in a freshwater lake with a UAS and a USV, and (2) compare in situ measurements of the dye from the USV to estimated concentrations of dye from UAS images. Here, we describe a series of field studies where a fluorescent dye (fluorescein) was released into a lake from an anchored floating platform. A fluorometer (fluorescence

sensor) was mounted underneath a USV, and was used to detect the released dye in situ. A UAS was used to visualize the dye and direct the USV to sample different areas of the plume. Existing image processing tools were used to map concentration profiles of the dye plume from stationary aerial images acquired from the UAS, and these were compared to concentration measurements collected from the sensors onboard the USV. The results of this project have the potential to transform monitoring strategies for hazardous agents, enabling timely cost effective, and accurate exposure assessment and response initiatives in affected areas. Fast response and versatile methods are essential in reacting to the introduction of hazardous agents, in order to quickly predict their spread and contain the event (Zou et al., 2016).

5.3 Materials and Methods

5.3.1 Study Site and Design

Field studies were conducted on 25 October, 2017 in a cove located at 37.053846, -80.640771 on Claytor Lake VA, USA (Figure 5.1). Claytor Lake is a 34 km long man-made reservoir with an approximate surface area of 18.2 square kilometers. Since the study was conducted in a small cove off the main body of the lake, this provided a natural isolated area to contain the dye and minimize interference from the general public. Though no permits were required to release the dye into Claytor Lake, local officials from Appalachian Power, Claytor Lake State Park, the Virginia Department of Game and Inland Fisheries, and the Friends of Claytor Lake were informed of our planned activities in advance of the dye release.

Field studies were performed from 1400 to 1500 EST. Twelve transects were performed by the USV across the dye plume. Two UAS missions were conducted (the flight time of the

UAS was limited to about 20 minutes for each mission). GPS of the UAS, USV, and the plume generator were recorded throughout the study. Meteorological data and fluorescein data were recorded at 1 Hz by the USV.

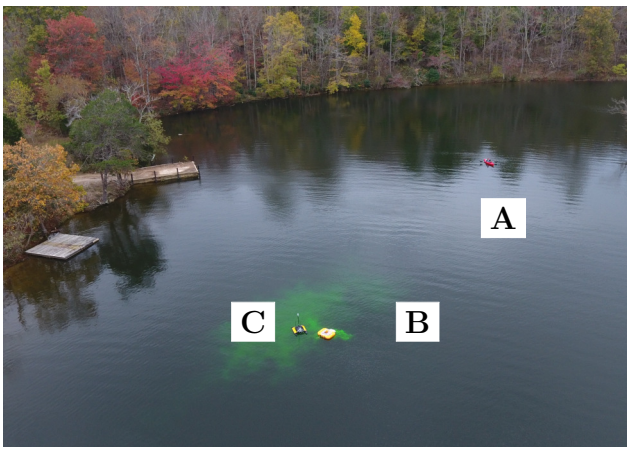

Figure 5.1: Site for study was a small cove in Claytor Lake, VA, USA. A kayak (A) was used to anchor a small float (B) near the center of the cove. A small fluorescein puck was placed in a mesh bag to create the plume. The USV (C) was equipped with an onboard fluorometer and was used to conduct a series of slow transects through the dye plume.

5.3.2 Unmanned Surface Vehicle

A Clearpath Robotics Kingfisher M200 USV (Clearpath Robotics, Kitchener, Ontario, Canada) was used to detect and track the dye (Figure 5.2). The Kingfisher USV weighed 28 kg, was 1.35 m x 0.98 m x 0.32 m (L x W x H), had a maximum payload of 10 kg, and was operated by remote control. The onboard computer as provided by the manufacturer was a Commell LE-376 (Commell IPC Division, Xizhi District, New Taipei City, Taiwan). The USV was powered by a removable 29 Ah battery with about three hours of continuous runtime at normal operation speeds. The propulsion system consisted of twin electric impeller thrusters, allowing a maximum speed of 1.7 m/s and steering with differential thrust. This configuration allowed for extremely precise, controlled movements and shallow operations

with minimal disturbance to the plume of the released dye. The live video feed from the UAS was used to guide the USV along the plume transects.

5.3.3 Unmanned Aircraft System

A DJI Phantom 4 (DJI, Shenzhen, China) UAS was used to capture 4K video and images of the dye plume and to provide visual navigation of the plume for the pilot of the USV. The Phantom 4 UAS weighed 1.38 kg, and was equipped with a gimbaled high definition camera. The camera was a 1/2.3" CMOS with a lens having 94° field of view, 20 mm f/2.8 focus at ∞. The UAS was launched and recovered from a manned pontoon boat anchored about 100 meters from the center of the dye release. The pilot-in-command (PIC, Schmale) was an FAA-certified remote pilot, Certificate Number 4038906. Raw data (e.g., GPS, timestamp, gimbal setting, etc.) associated with the images captured with the UAS are provided as a supplemental spreadsheet file to this manuscript.

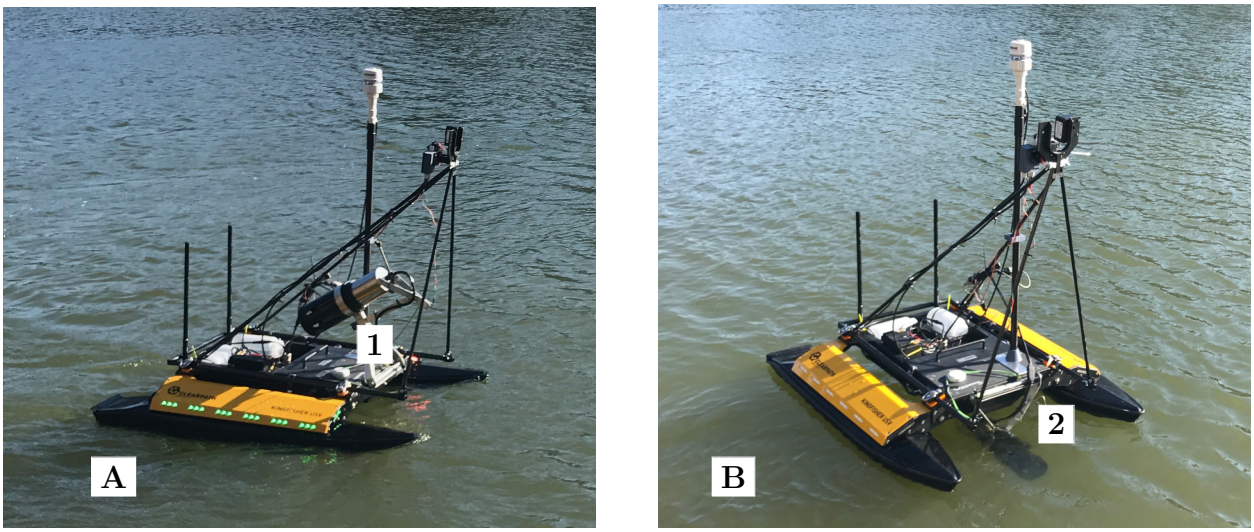

Figure 5.2: Clearpath Robotics M200 Kingfisher with the Turner C6 multisensor in the upright and stowed configuration (A,1) and deployed for taking dye measurements near the water surface (B,2). The C6 sensor array can use up to six sensors to simultaneously take environmental measurements such as turbidity and fluorescence.

5.3.4 Sensor Integration

A Turner Designs C6 multi-sensor platform (Turner Designs, San Jose, CA, USA) was used for fluorescein concentration measurements. The C6 sensor array accepts up to six individual fluorescence and turbidity sensors. The sensor weighed 2.74 kg and was 33.8 cm x 10.2 cm (L x D). The C6 can be operated at depths down to 600 m and from -2 to 50 degrees C (as per the manufacturer specifications). In our studies, the C6 was used to measure depth (pressure), water temperature, turbidity (Model #2100-000-T), and fluorescein (Model #2100-000-F). A mounting system was developed for the C6 sensor to allow the sensor to operate 16cm below the water surface when deployed (Figure 5.2). The sensor was located in the middle and slightly aft of the pontoon mid-point. The mounting system allowed for the sensor to be folded up and out of the water for transport and launching (Figure 5.2). The C6 unit was used to calibrate the turbidity sensor in a 2L solution of 50 NTU Turbidity Standard (StablCal #26606-49, Cole Parmer, Vernon Hills, IL, 60061) The fluorescein sensor was calibrated with the C6 unit in 2 L of a 40 PPB solution (Fluorescein 400 PPB #10-509, Turner Designs, San Jose, CA 95112). Calibrations were carried out in the lab by submerging the entire C6 unit and casing into a container wrapped in a black velvet cloth to eliminate light during calibration. The installed sensors for Turbidity and Fluorescein were calibrated with with the C6 sensor suite on October 24, 2017. The Turbidity sensor had a blank background RFU value of 17.64 in distilled water, and a working RFU value of 1279.60 in a standard solution of 50 NTU. The Standard RFU for this experimental data was set to 1280.80 with background Blank RFU values for the calibration at 288.00, 41.20, and 17.36 for the predetermined gain values of x1, x10, x100, respectively. The Fluorescein sensor had a working RFU value of 3833.60 in a standard solution of 40 ppb. The Standard RFU for this experimental data was set to 3834.00 with background Blank RFU values for the calibration at 284.00, 33.20, and 8.64 for the predetermined gain values of x1, x10, x100, respectively.

An Airmar 200WX meteorological sensor (Airmar Technology Corporation, Milford, NH, USA) was used for environmental measurements such as wind speed, wind direction, air temperature and atmospheric pressure (Figure 5.2). Both sensors were connected to the onboard USV computer for data collection and recording.

5.3.5 Plume Generation

A fluorescein puck (Bright Dyes yellow/green cake cat #102001, Kingscote Chemicals, Miamisburg, OH 45342) weighing 56.14 g was used to generate the dye plume. The fluorescein puck was suspended underwater from an Intex cooler float (Intex Recreation Corp., Long Beach, CA, USA) in a mesh bag at a depth of 67 cm. The float was anchored in place (37.0535180,-80.6427000) with a 4.5 kg Greenfield Products anchor. The 30 cm anchor rested on the bottom of the lake and was attached to 10 m of 5/8 cm utility line. The puck was allowed to disperse fluorescein by diffusion only (i.e., the dye was not forcibly released, and there were no currents in the lake). The movement of the float by wind interaction aided in dispersion of the tracer dye. Tracking of this motion was not recorded.

5.3.6 Image Processing

Image processing was completed using ImageMagick version 6.8.9-9 and Gimp version 2.8.16 software. Images were used over video for ease of analysis, in particular for lower computational cost needed for future live UAS image processing. Images were 2400 $\times$ 1800 (W $\times$ H) in size. Images were captured from 25 m at approximately one image for every 3 seconds. Pixel sizes were 1.5 cm in length. Enhanced color reference images were created using Gimp by adjusting the red, green and blue (RGB) levels to the values in (Figure 5.3), in order to increase the dye plume contrast (shown in Figure 5.3) to aid in visual identification of plume

concentration structures.

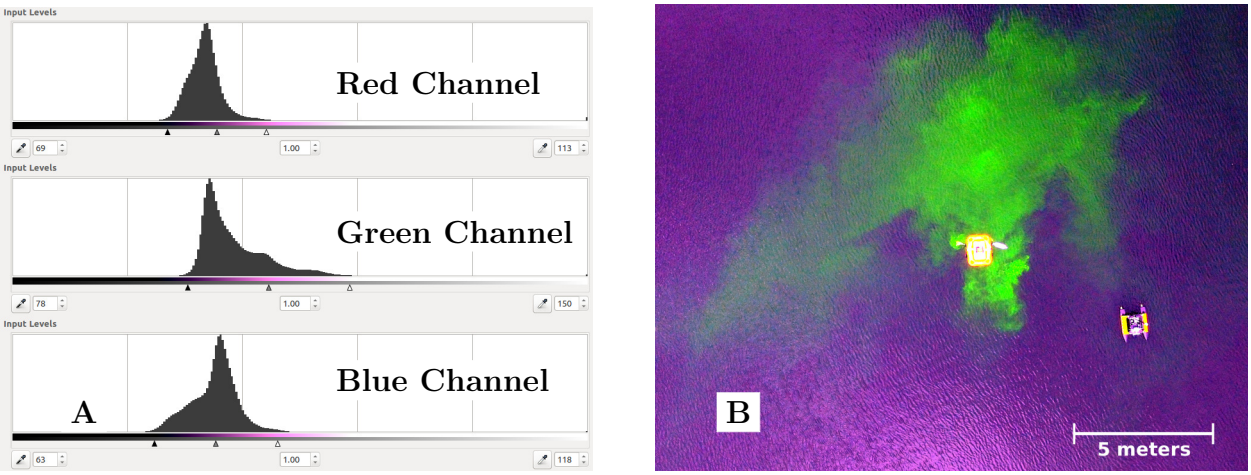

Figure 5.3: RGB channel levels after adjustment of raw fluorescein plume images taken from the UAS to increase color contrast of plume structure (A), creating an enhanced color rendering of the fluorescein plume revealing concentration structures not seen in the raw images (B).

The convert function from ImageMagick (command line operation), was used on the raw images to create color maps known as heatmaps by assigning a chosen color (heat) to represent a change in concentration. Heatmaps were generated by converting image pixels matching (by percentage of maximum possible color intensity) the fluorescein dye color represented by the RGB value (100,200,60) to the chosen heatmap colors. Percentages ranged from 13 % to 23 % in 2 % increments, representing red, yellow, green, cyan, blue, and black respectively (Figure 5.5), and were assigned decreasing parts per million (PPM) values based on minimum and maximum concentrations from the USV fluorescein sensor. The color white represented 12 ppm where percentage of maximum possible intensity was from 0 % to 12.9 % and was matched to the maximum concentration recorded by the USV fluorescein sensor. A scale of 2 ppm per increase in heatmap concentration was used with the exception of 1 ppm. Exchangeable image file format (EXIF) data from UAS imagery was used to rename the images by timestamp and to connect with USV data.

5.4 Results and Discussion

A series of field studies were conducted to track a fluorescent dye released into a lake from an anchored floating platform. A UAS was used to visualize the dye and direct the USV to sample different areas of the plume. Image processing tools were used to map concentration profiles of the dye plume from aerial images acquired from the UAS, and these were compared to concentration measurements collected from the sensors onboard the USV. In situ fluorescein concentration profiles measured with the USV were similar to the intensity of the plume as seen by raw images from the UAS (Figure 5.4). Color enhanced images revealed subtle differences in concentrations not seen in the raw images (such as Figure 5.3). For the transect shown by the white line in (Figure 5.5), we assigned concentrations to color values (heat) to the raw image based on the minimum and maximum values recorded by the Turner C6 sensor on the USV. Plot points for time were chosen according to when the USVs path was in the midpoint between the discretized concentration boundaries represented by the colors of the heatmap. This was then compared to the Turner C6 concentrations recorded for the transect shown in (Figure 5.6). The shape of both curves in Figure 5.6 were similar, demonstrating that the processed images from the UAS could be used to accurately predict dye concentrations near the water surface (i.e., the USV provided the ground-truthing needed to validate these image predictions).

Hazardous agent spills represent an important economic and health cost to the global community. There are knowledge gaps in understanding the transport of these agents in aquatic environments such as the fate and transport of spilled oil (Gong et al., 2014). The coordinated aspect of this study provides a base for future development of completely autonomous multifaceted hazardous plume concentration measurements. The technologies used and the techniques developed in this study could eventually be used to provide comprehensive spatial and temporal maps of hazardous plume concentrations. Though typical measurements of

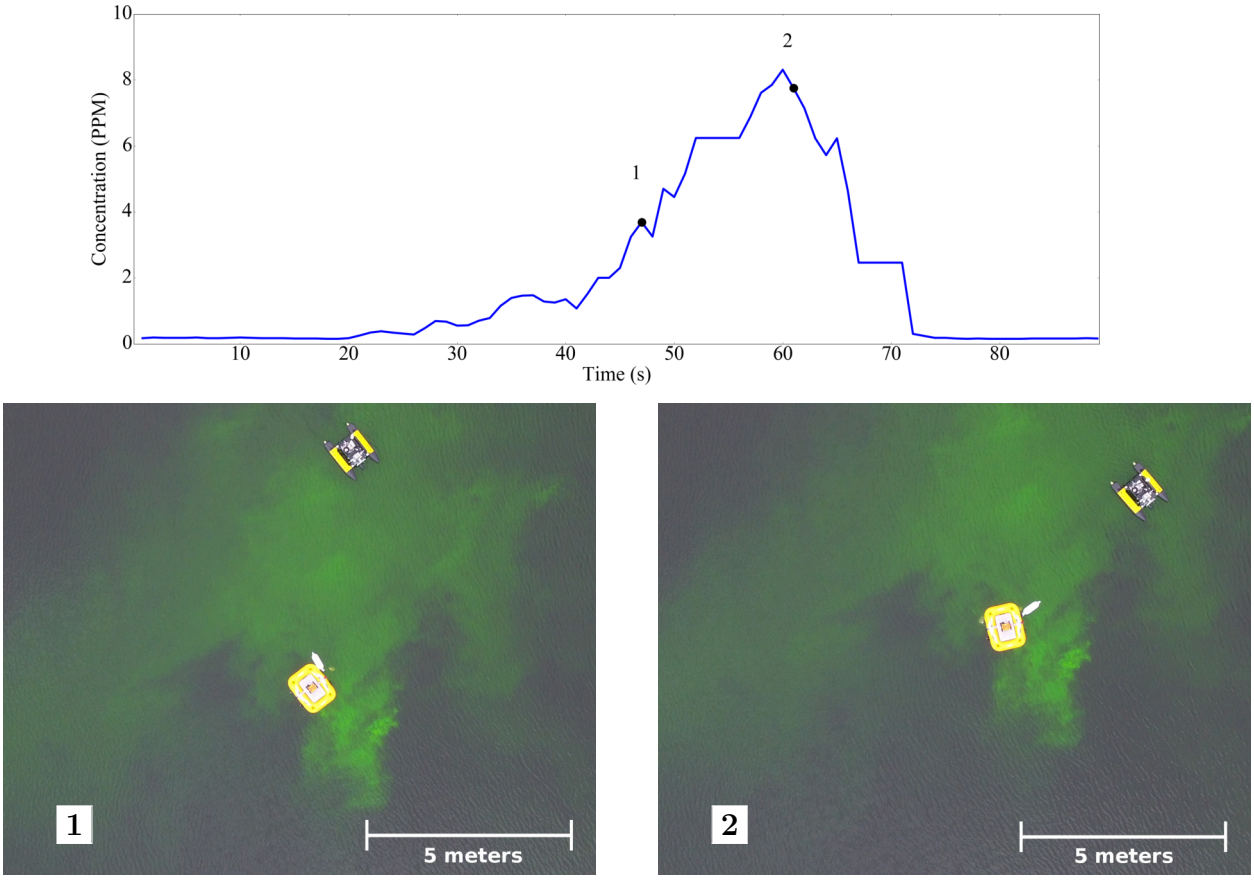

Figure 5.4: Fluorescein concentration profile as recorded by the Turner C6 equipped USV. Concentration is increasing from location 1 to 2 and then decreasing as the USV traverses the dye plume for a single transect.

agents such as HABs are made using satellite imagery, these measurements can be prone to errors when the water surface turbulence is large enough (Klemas, 2011) and may need in situ measurements (ground-truthing) to calibrate the measurements (Carvalho et al., 2011). Moreover, some types (species) of HABs are not detectable by satellite imagery (Tang et al., 2003). Coordinated systems of autonomous unmanned vehicles could be used to patrol coast lines to help identify HABs before they become large and dangerous.

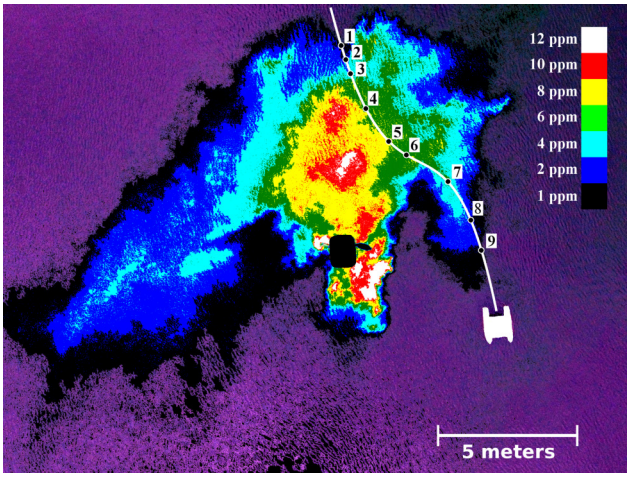

Figure 5.5: Heatmap of fluorescein concentration profile using color matching technique. White represents areas of the highest concentrations (12 ppm) with black representing the lowest concentration (1 ppm). The path of the USV is represented by the white curved line (points 1 to 9) with the plume generation float seen as the black rectangular object in the plume.

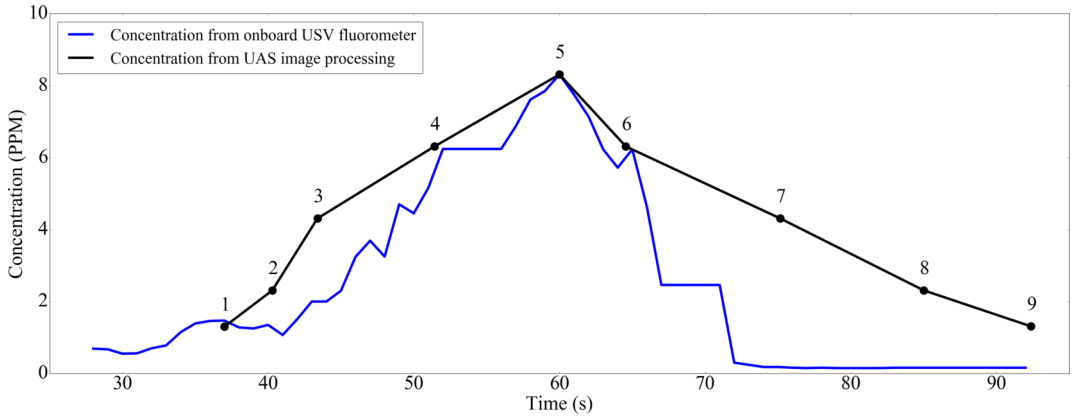

Figure 5.6: Fluorescein concentration profile from the Turner C6 sensor (Blue) onboard the USV, and an estimated concentration profile from the heat map for the same plume transect. Points 1 to 9 represent the midpoint of each concentration level from the heatmap as the USV performed the transect.

Though our coordination of unmanned systems provided a good agreement in concentrations from aerial optical measurements with near surface fluorescein concentration measurements (Figure 5.6), some slight deviations could be observed. First, some of the error in the comparison of the in situ dye detection and the heat maps of concentrations extracted from the digital images could be partially eliminated by using Real Time Kinematic GPS systems in the future. This GPS technology can map locations as small as 2 cm and could account for changes in the speed of the USV that was not accounted for in our study and would help localize concentration measurements from the USV both temporally and spatially. Second, errors might also be explained by changes of speed of the USV which could skew a concentration profile. It's also important to note that the visual surface concentration will not completely match the concentration measurements from the Turner C6 sensor due to the 16 cm depth the sensor was operated. Using a finer scale conversion of color matching to create heatmaps would lead to higher resolution concentration profiles to aid in automated image validation however, a finer scale is not needed for visual inspection. Spectral and radiometric calibrations of the UAS camera is also needed to increase both accuracy and precision of the image processing. Moreover, accounting for more image property variables such as brightness

and hue and using turbidity data could also lead to more accurate heatmaps with a better understanding of how much depth from the surface impacts the visual based concentration profiles. Future studies are also needed to elucidate minimum concentrations that can be mapped by a UAS and to monitor actual concentrations of dye using color intensity (compared to relative concentrations used in this study). Eliminating the manned component as a next step could remove additional error by using precise command and control algorithms that manned control cannot duplicate. Direct UAS to USV communication coordination as a type of heterogeneous swarm (Szwaykowska et al., 2015) could allow for highly efficient search and mapping of dyes and hazardous agents in the future.

5.5 Conclusions

A fluorescent dye was released into a freshwater lake from an anchored floating platform. A fluorometer was mounted underneath a USV, and was used to detect and track the released dye in situ in real-time. A UAS was used to visualize the dye and direct the USV to sample different areas of the dye plume. Image processing tools were used to map concentration profiles of the dye plume from aerial images acquired from the UAS, and these were associated with concentration measurements collected from the sensors onboard the USV. In situ fluorescein concentration profiles measured with the USV were similar to the intensity of the plume as seen by raw images from the UAS. Color-enhanced images revealed subtle differences in concentrations not seen in the raw images. The concentration profiles revealed from the USV and UAS were similar, demonstrating that the processed images from the UAS could be used to accurately predict dye concentrations near the water surface.

This work establishes the concepts and techniques needed to use coordinate unmanned systems to safely and cost effectively identify and map hazardous agents. Additionally with

further development, this work can be adapted to allow the UAS to work individually to locate and quantify hazardous agents when ocean conditions are prohibitive for USV operations. Hazardous agents represent a hazard to marine resources and human health and effect the economies of most coastal communities. Using these systems and techniques, or variations of the systems and techniques developed in this work, could provide a fast tool to identify and localize hazardous agents in the future.

5.6 Acknowledgements

This research was supported in part by the National Science Foundation (NSF) under Grant Numbers DGE-0966125 (IGERT: MultiScale Transport in Environmental and Physiological Systems (MultiSTEPS)), AGS 1520825 (Hazards SEES: Advanced Lagrangian Methods for Prediction, Mitigation and Response to Environmental Flow Hazards), and IIS-1637915 (NRI: Coordinated Detection and Tracking of Hazardous Agents with Aerial and Aquatic Robots to Inform Emergency Responders). Any opinions, findings, and conclusions or recommendations expressed in this material are those of the authors and do not necessarily reflect the views of the NSF.

Chapter 6. Conclusions

6.1 Implications and Future Work

Additional field studies using the unmanned systems and sensors developed for this research are recommended to develop the needed historical data to make observations on the transport of microorganisms across different temporal and spatial scales. Understanding the spatial distribution of these microorganisms in a large freshwater lake such as Claytor Lake, requires a long term commitment (missions across several years) to data collection. The mixing and concentration of microorganisms are influenced by many factors such as temperature, lake turnover (Yu et al., 2014) and ultimately seasons (Pietsch et al., 2017). Stationary versions of these sensors, placed in moored buoys in the water and on towers over land for example, could be used to collect some of these data such as wind speed and direction, humidity, temperature and turbidity. The inclusion of particle counters would help to identify daily particle count fluctuations for both biotic and abiotic aerosols. Many locations around the world have such sensors in place currently reporting air quality such as the air quality index (AQI) in China (Jiang et al., 2015). Impingers and deposition devices (e.g., Petri plates or Burkard volumetric samplers) could assist in the identification of microbes in the samples. The recent appearance and rapid growth of tools such as 3D printers allow for small scale manufacture of extremely affordable and effective alternatives to commercial sensors that

allow these tools to be used en masse on large scales.

Further use of optical particle sensors in this field of research should be backed up by lab experiments to help understand the usefulness of these sensors in aquatic environments. It is known that extremely humid air can increase the measured size of particles up substantially (Silva et al., 2015). In some cases, hygroscopic aerosols can double in diameter(Schumann, 1990). Quantifying this effect for the particular sensors used and particular aerosols of interest is essential to resolve and identify actual particle diameters. Characterizing the measurement of abiotic particulates such as sea salt, other inorganic compounds and ultra-fine water droplets by these sensors is another important aspect needed to use these sensors in particular environments. In some locations, sea salt alone accounted for approximately 15% of the total aerosols for particulates less than 1µm (Vogt et al., 2013). Lab based studies could help develop models useful for removing these unwanted measured particles as background noise making the particulate data more useful.

The simultaneous atmospheric sampling from a USV and UAV in this research exhibit the usefulness and need for heterogeneous teams of unmanned vehicles to accomplish certain research tasks that otherwise would be a challenge to conduct with manned operations. Heterogeneous systems are currently being developed and tested (Duan and Liu, 2010; Palacios et al., 2017). These systems are complex in their nature, but are powerful scientific tools useful to fields outside of engineering. It is recommended that the use of cooperative unmanned systems be extended even further to collect the necessary large scale data to help understand and predict bacterial populations in and above aquatic environments. One could envision swarms of USVs, UASs, and UGVs operationg simultaneosly across land, air, and water. The development of low cost unmanned systems is becoming more common (Hoffer et al., 2014) and the autonomous nature of these systems can be exploited without costly investment both in time and equipment. Heterogeneous swarm capabilities are not new (Chung et al., 2011),

and have been demonstrated by Duan et al (Duan et al., 2011) and others (Luo and Duan, 2013). A combination of UAVs, USVS, UGVs, and remotely operated underwater vehicles (ROVs) could be used to gather samples from water and the atmosphere in groups over large areas in terrestrial, aquatic and atmospheric environments. This data would give context to and connect the many current small scale environmental research endeavors. Detailed models could be developed from this data and used to help understand current bacterial populations and help predict their transport and effect on important economic crops and related weather.

Sensors that were developed and integrated into the unmanned systems for this research could be expanded. A low cost direct to plate deposition system was developed during this research and could be used to augment the use of impingers on USVs (Appendix). Additional sensors such as surface plasmon resonance (SPR) which have been used on UAV previously (Palframan et al., 2014) to detect and differentiate different species of bacteria (Adducci et al., 2016), could be adapted to detect specific biological agents and used to direct the coordinated sampling of unmanned vehicles to identify and localize sources. The additional sensors would be used in this special case for verification and quantification of these agents. The use of a turbidity sensor while tracking plumes could be used to quantify the maximum depth of resolved concentrations in heatmaps developed from aerial images. The development and integration of new low cost sensors to be used in large heterogeneous swarms of UVs is an exciting and powerful new path for scientific exploration that could help to reveal large scale relationships and models for complex biological dynamics.

Bibliography

Adducci, B. A., Gruszewski, H. A., Khatibi, P. A., and Schmale, D. G. (2016). Differential detection of a surrogate biological threat agent (bacillus globigii) with a portable surface plasmon resonance biosensor. *Biosensors and Bioelectronics*, 78:160–166.

Alpert, P. A., Kilthau, W. P., Bothe, D. W., Radway, J. C., Aller, J. Y., and Knopf, D. A. (2015). The influence of marine microbial activities on aerosol production: A laboratory mesocosm study. *Journal of Geophysical Research: Atmospheres*, 120(17):8841–8860.

Anderson, D., Keafer, B., Geyer, W., Signell, R., and Loder, T. (2005). Toxic alexandrium blooms in the western gulf of maine: The plume advection hypothesis revisited. *Limnology and Oceanography*, 50(1):328–345.

Arifianto, O. and Farhood, M. (2015). Development and modeling of a low-cost unmanned aerial vehicle research platform. *Journal of Intelligent & Robotic Systems*, 80(1):139.

Arnon, A., Lensky, N., and Selker, J. (2014a). High-resolution temperature sensing in the dead sea using fiber optics. *Water Resources Research*, 50(2):1756–1772.

Arnon, A., Selker, J., and Lensky, N. (2014b). Correcting artifacts in transition to a wound optic fiber: Example from high-resolution temperature profiling in the dead sea. *Water Resources Research*, 50(6):5329–5333.

Bakker, M., Caljé, R., Schaars, F., van der Made, K.-J., and de Haas, S. (2015). An active heat tracer experiment to determine groundwater velocities using fiber optic cables installed with direct push equipment. *Water Resources Research*, 51(4):2760–2772.

Bamberger Jr, R. J., Watson, D. P., Scheidt, D. H., and Moore, K. L. (2006). Flight demonstrations of unmanned aerial vehicle swarming concepts. *Johns Hopkins APL Technical Digest*, 27(1):41–55.

Bandini, F., Butts, M., Jacobsen, T. V., and Bauer-Gottwein, P. (2017a). Water level observations from unmanned aerial vehicles for improving estimates of surface water–groundwater interaction. *Hydrological Processes*, 31(24):4371–4383.

Bandini, F., Jakobsen, J., Olesen, D., Reyna-Gutierrez, J. A., and Bauer-Gottwein, P. (2017b). Measuring water level in rivers and lakes from lightweight unmanned aerial vehicles. *Journal of Hydrology*, 548:237–250.

Barczewski, B. and Marschall, P. (1990). Develpment of a lightfibre lluorometer for in-situ tracer concentration measurements.

Bauer, H., Kasper-Giebl, A., Löflund, M., Giebl, H., Hitzenberger, R., Zibuschka, F., and Puxbaum, H. (2002). The contribution of bacteria and fungal spores to the organic carbon content of cloud water, precipitation and aerosols. *Atmospheric Research*, 64(1):109–119.

Beisner, B. E., Peres-Neto, P. R., Lindström, E. S., Barnett, A., and Longhi, M. L. (2006). The role of environmental and spatial processes in structuring lake communities from bacteria to fish. *Ecology*, 87(12):2985–2991.

Blanchard, D. C. (1989). The ejection of drops from the sea and their enrichment with bacteria and other materials: a review. *Estuaries and Coasts*, 12(3):127–137.

Bond, R. M., Stubblefield, A. P., and Van Kirk, R. W. (2015). Sensitivity of summer stream temperatures to climate variability and riparian reforestation strategies. *Journal of Hydrology: Regional Studies*, 4:267–279.

Briggs, M. A., Lautz, L. K., McKenzie, J. M., Gordon, R. P., and Hare, D. K. (2012). Using high-resolution distributed temperature sensing to quantify spatial and temporal variability in vertical hyporheic flux. *Water Resources Research*, 48(2).

Burrows, S., Butler, T., Jöckel, P., Tost, H., Kerkweg, A., Pöschl, U., and Lawrence, M. (2009). Bacteria in the global atmosphere–part 2: Modeling of emissions and transport between different ecosystems. *Atmospheric Chemistry and Physics*, 9(23):9281–9297.

Buzatu, D. A., Moskal, T. J., Williams, A. J., Cooper, W. M., Mattes, W. B., and Wilkes, J. G. (2014). An integrated flow cytometry-based system for real-time, high sensitivity bacterial detection and identification. *PloS one*, 9(4):e94254.

Carvalho, G. A., Minnett, P. J., Banzon, V. F., Baringer, W., and Heil, C. A. (2011). Long-term evaluation of three satellite ocean color algorithms for identifying harmful algal blooms (karenia brevis) along the west coast of florida: A matchup assessment. *Remote sensing of environment*, 115(1):1–18.

Cherrie, J., Howie, R., and Semple, S. (2011). *Monitoring for health hazards at work*. John Wiley & Sons.

Christner, B. C., Cai, R., Morris, C. E., McCarter, K. S., Foreman, C. M., Skidmore, M. L., Montross, S. N., and Sands, D. C. (2008a). Geographic, seasonal, and precipitation chemistry influence on the abundance and activity of biological ice nucleators in rain and snow. *Proceedings of the National Academy of Sciences*, 105(48):18854–18859.

Christner, B. C., Morris, C. E., Foreman, C. M., Cai, R., and Sands, D. C. (2008b). Ubiquity of biological ice nucleators in snowfall. *Science*, 319(5867):1214–1214.

Chung, H., Oh, S., Shim, D. H., and Sastry, S. S. (2011). Toward robotic sensor webs: Algorithms, systems, and experiments. *Proceedings of the IEEE*, 99(9):1562–1586.

Cinotto, P. J. (2005). *Occurrence of fecal-indicator bacteria and protocols for identification of fecal-contamination sources in selected reaches of the West Branch Brandywine Creek, Chester County, Pennsylvania*. US Department of the Interior, US Geological Survey.

Clarkson, M., Kasemann, S., Wood, R., Lenton, T., Daines, S., Richoz, S., Ohnemueller, F., Meixner, A., Poulton, S., and Tipper, E. (2015). Ocean acidification and the permo-triassic mass extinction. *Science*, 348(6231):229–232.

Cohen, A., Anderson, H., Ostro, B., Pandey, K., Krzyzanowski, M., Kunzli, N., Gutschmidt, K., Pope III, C., Romieu, I., and Samet, J. (2001). Urban air pollution: Comparative quantification of health risks. *World Health Organization*.

Colbeck, I. et al. (2014). *Aerosol Science: Technology and Applications*. John Wiley & Sons.

Cook, S. A. (1983). An overview of computational complexity. *Communications of the ACM*, 26(6):400–408.

Cox, C. S. and Wathes, C. M. (1995). *Bioaerosols handbook*. crc press.

Cruz, N. A. and Matos, A. C. (2010). Adaptive sampling of thermoclines with autonomous underwater vehicles. In *OCEANS 2010*, pages 1–6. IEEE.

Csanady, G. T. (1973). The fluctuation problem in turbulent diffusion. In *Turbulent Diffusion in the Environment*, pages 222–248. Springer.

Davies-Colley, R., Nagels, J., Donnison, A., and Muirhead, R. (2004). Flood flushing of bugs in agricultural streams. *Water and Atmosphere*, 12(2):18–20.

De Jong, S., Slingerland, J., and Van de Giesen, N. (2015). Fiber optic distributed temperature sensing for the determination of air temperature. *Atmospheric Measurement Techniques*, 8(1):335–339.

Demir, K. A., Cicibas, H., and Arica, N. (2015). Unmanned aerial vehicle domain: Areas of research. *Defence Science Journal*, 65(4).

Detert, M. and Weitbrecht, V. (2015). A low-cost airborne velocimetry system: proof of concept. *Journal of Hydraulic Research*, 53(4):532–539.

Duan, H. and Liu, S. (2010). Unmanned air/ground vehicles heterogeneous cooperative techniques: Current status and prospects. *Science China Technological Sciences*, 53(5):1349–1355.

Duan, H., Zhang, Y., and Liu, S. (2011). Multiple UAVs/ugvs heterogeneous coordinated technique based on receding horizon control (rhc) and velocity vector control. *Science China Technological Sciences*, 54(4):869–876.

Duarte, M., Costa, V., Gomes, J., Rodrigues, T., Silva, F., Oliveira, S. M., and Christensen, A. L. (2016). Evolution of collective behaviors for a real swarm of aquatic surface robots. *PloS one*, 11(3):e0151834.

Dunbabin, M. and Marques, L. (2012). Robots for environmental monitoring: Significant advancements and applications. *IEEE Robotics & Automation Magazine*, 19(1):24–39.

Failor, K., Schmale 3rd, D., Vinatzer, B., and Monteil, C. (2017). Ice nucleation active bacteria in precipitation are genetically diverse and nucleate ice by employing different mechanisms. *The ISME journal*.

Faizal, M. and Rafiuddin Ahmed, M. (2011). On the ocean heat budget and ocean thermal energy conversion. *International Journal of Energy Research*, 35(13):1119–1144.

Fay, J. A. (2003). Model of spills and fires from lng and oil tankers. *Journal of Hazardous Materials*, 96(2):171–188.

Fiedler, P. C. (2010). Comparison of objective descriptions of the thermocline. *Limnology and Oceanography: Methods*, 8(6):313–325.

Flickenger, R., Okay, S., Pietrosemoli, E., Zennaro, M., and Fonda, C. (2008). Very long distance wi-fi networks. In *Proceedings of the second ACM SIGCOMM workshop on Networked systems for developing regions*, pages 1–6. ACM.

Fröhlich-Nowoisky, J., Kampf, C. J., Weber, B., Huffman, J. A., Pöhlker, C., Andreae, M. O., Lang-Yona, N., Burrows, S. M., Gunthe, S. S., Elbert, W., et al. (2016). Bioaerosols in the earth system: Climate, health, and ecosystem interactions. *Atmospheric Research*, 182:346–376.

Funkhouser, J. E. and Barks, C. S. (2004). Development of a traveltime prediction equation for streams in arkansas. Technical report.

Galland, F., Réfrégier, P., and Germain, O. (2004). Synthetic aperture radar oil spill segmentation by stochastic complexity minimization. *IEEE Geoscience and Remote Sensing Letters*, 1(4):295–299.

Garbe, C. S., Handler, R. A., and Jähne, B. (2014). *Transport at the Air-sea Interface*. Springer.

Garratt, J. R. (1994). The atmospheric boundary layer. *Earth-Science Reviews*, 37(1-2):89–134.

Ghani, M. H., Hole, L. R., Fer, I., Kourafalou, V. H., Wienders, N., Kang, H., Drushka, K., and Peddie, D. (2014). The sailbuoy remotely-controlled unmanned vessel: measurements of near surface temperature, salinity and oxygen concentration in the northern gulf of mexico. *Methods in Oceanography*, 10:104–121.

Gong, Y., Zhao, X., Cai, Z., O'reilly, S., Hao, X., and Zhao, D. (2014). A review of oil, dispersed oil and sediment interactions in the aquatic environment: influence on the fate, transport and remediation of oil spills. *Marine pollution bulletin*, 79(1):16–33.

Gras, J. L. and Keywood, M. (2017). Cloud condensation nuclei over the southern ocean: wind dependence and seasonal cycles. *Atmospheric Chemistry and Physics*, 17(7):4419–4432.

Gunatilaka, A., Skvortsov, A., and Gailis, R. (2012). High fidelity simulation of hazardous plume concentration time series based on models of turbulent dispersion. In *Information Fusion (FUSION), 2012 15th International Conference on*, pages 1838–1845. IEEE.

Hallar, A., Huffman, J. A., and Fridlind, A. (2012). Biological aerosol effects on clouds and precipitation. *Eos, Transactions American Geophysical Union*, 93(51):539–539.

Handler, R., Smith, G., and Leighton, R. (2001). The thermal structure of an air–water interface at low wind speeds. *Tellus A*, 53(2):233–244.

Hanlon, R., Powers, C., Failor, K., Monteil, C. L., Vinatzer, B. A., and Schmale, D. G. (2017). Microbial ice nucleators scavenged from the atmosphere during simulated rain events. *Atmospheric Environment*.

Hausner, M. B., Suárez, F., Glander, K. E., Giesen, N. v. d., Selker, J. S., and Tyler, S. W. (2011). Calibrating single-ended fiber-optic raman spectra distributed temperature sensing data. *Sensors*, 11(11):10859–10879.

Hilgersom, K., van Emmerik, T., Solcerova, A., Berghuijs, W., Selker, J., and van de Giesen, N. (2016). Practical considerations for enhanced-resolution coil-wrapped distributed temperature sensing.

Hill, T. C., Moffett, B. F., DeMott, P. J., Georgakopoulos, D. G., Stump, W. L., and Franc, G. D. (2014). Measurement of ice nucleation-active bacteria on plants and in precipitation by quantitative PCr. *Applied and environmental microbiology*, 80(4):1256–1267.

Hirano, S. S. (1995). Ecology of ice nucleation-active bacteria. *Biological ice nucleation and its applications*, pages 41–61.

Hockett, K. L., Burch, A. Y., and Lindow, S. E. (2013). Thermo-regulation of genes mediating motility and plant interactions in pseudomonas syringae. *PLoS One*, 8(3):e59850.

Hoffer, N. V., Coopmans, C., Jensen, A. M., and Chen, Y. (2014). A survey and categorization of small low-cost unmanned aerial vehicle system identification. *Journal of Intelligent & Robotic Systems*, 74(1-2):129.

Humayoun, S. B., Bano, N., and Hollibaugh, J. T. (2003). Depth distribution of microbial diversity in mono lake, a meromictic soda lake in california. *Applied and environmental microbiology*, 69(2):1030–1042.

Ichinose, Y., Taguchi, F., and Mukaihara, T. (2013). Pathogenicity and virulence factors of pseudomonas syringae. *Journal of general plant pathology*, 79(5):285–296.

Jackson, P. R. and Lageman, J. D. (2013). Real-time piscicide tracking using rhodamine wt dye for support of application, transport, and deactivation strategies in riverine environments. Technical report, US Geological Survey.

Jiang, W., Wang, Y., Tsou, M.-H., and Fu, X. (2015). Using social media to detect outdoor air pollution and monitor air quality index (aqi): a geo-targeted spatiotemporal analysis framework with sina weibo (chinese twitter). *PloS one*, 10(10):e0141185.

JONES IV, G. P., Pearlstine, L. G., and Percival, H. F. (2006). An assessment of small unmanned aerial vehicles for wildlife research. *Wildlife Society Bulletin*, 34(3):750–758.

Jonsson, P., Olofsson, G., and Tjärnhage, T. (2014). *Bioaerosol detection technologies*. Springer.

Kersey, A. D. (2000). Optical fiber sensors for permanent downwell monitoring applications in the oil and gas industry. *IEICE transactions on electronics*, 83(3):400–404.

Kim, J.-W., Pachepsky, Y. A., Shelton, D. R., and Coppock, C. (2010). Effect of streambed bacteria release on e. coli concentrations: Monitoring and modeling with the modified swat. *Ecological Modelling*, 221(12):1592–1604.

Kimmel, B. L. and Groeger, A. W. (1984). Factors controlling primary production in lakes and reservoirs: a perspective. *Lake and reservoir management*, 1(1):277–281.

Kingston, P. F. (2002). Long-term environmental impact of oil spills. *Spill Science & Technology Bulletin*, 7(1):53–61.

Kinsman, B. (1965). *Wind waves: their generation and propagation on the ocean surface*. Courier Corporation.

Klemas, V. (2011). Remote sensing of algal blooms: an overview with case studies. *Journal of Coastal Research*, 28(1A):34–43.

Kolling, A., Walker, P., Chakraborty, N., Sycara, K., and Lewis, M. (2016). Human interaction with robot swarms: A survey. *IEEE Transactions on Human-Machine Systems*, 46(1):9–26.

Kuwata, Y., Wolf, M. T., Zarzhitsky, D., and Huntsberger, T. L. (2014). Safe maritime autonomous navigation with colregs, using velocity obstacles. *IEEE Journal of Oceanic Engineering*, 39(1):110–119.

Latif, M., Böning, C., Willebrand, J., Biastoch, A., Dengg, J., Keenlyside, N., Schweckendiek, U., and Madec, G. (2006). Is the thermohaline circulation changing? *Journal of Climate*, 19(18):4631–4637.

Lauffenburger, D. A. (1991). Quantitative studies of bacterial chemotaxis and microbial population dynamics. *Microbial Ecology*, 22(1):175–185.

Laut, J., Henry, E., Nov, O., and Porfiri, M. (2014a). Development of a mechatronics-based citizen science platform for aquatic environmental monitoring. *IEEE/ASME Transactions on Mechatronics*, 19(5):1541–1551.

Laut, J., Wright, S. N., Nov, O., and Porfiri, M. (2014b). Gowanus voyage: where mechatronics, public art, community members, and environmental science meet [focus on education]. *IEEE Control Systems*, 34(1):60–64.

Law, C. and Khoo, B. (2002). Transport across a turbulent air-water interface. *AIChE Journal*, 48(9):1856–1868.

Lee, S.-A., Adhikari, A., Grinshpun, S. A., McKay, R., Shukla, R., and Reponen, T. (2006). Personal exposure to airborne dust and microorganisms in agricultural environments. *Journal of occupational and environmental hygiene*, 3(3):118–130.

Lewitus, A. J., Horner, R. A., Caron, D. A., Garcia-Mendoza, E., Hickey, B. M., Hunter, M., Huppert, D. D., Kudela, R. M., Langlois, G. W., Largier, J. L., et al. (2012). Harmful algal blooms along the North American west coast region: History, trends, causes, and impacts. *Harmful algae*, 19:133–159.

Li, M., Yu, X., Kang, H., Xie, Z., and Zhang, P. (2017). Concentrations and size distributions of bacteria-containing particles over oceans from China to the arctic ocean. *Atmosphere*, 8(5):82.

Li, W., Farrell, J. A., Pang, S., and Arrieta, R. M. (2006). Moth-inspired chemical plume tracing on an autonomous underwater vehicle. *IEEE Transactions on Robotics*, 22(2):292–307.

Lien, F.-S., Ji, H., and Yee, E. (2007). Computational modeling of aerosol hazard arising from the opening of an anthrax letter in an open-office complex. In *New Trends in Fluid Mechanics Research*, pages 407–410. Springer.

Lin, X., Reponen, T. A., Willeke, K., Grinshpun, S. A., Foarde, K. K., and Ensor, D. S. (1999). Long-term sampling of airborne bacteria and fungi into a non-evaporating liquid. *Atmospheric Environment*, 33(26):4291–4298.

Lin, X., Willeke, K., Ulevicius, V., and Grinshpun, S. A. (1997). Effect of sampling time on the collection efficiency of all-glass impingers. *American Industrial Hygiene Association Journal*, 58(7):480–488.

Lindström, E. S., Kamst-Van Agterveld, M. P., and Zwart, G. (2005). Distribution of typical freshwater bacterial groups is associated with ph, temperature, and lake water retention time. *Applied and environmental microbiology*, 71(12):8201–8206.

Liu, Y. and Minnett, P. J. (2016). Sampling errors in satellite-derived infrared sea-surface temperatures. part i: Global and regional modis fields. *Remote Sensing of Environment*, 177:48–64.

Luo, Q. and Duan, H. (2013). An improved artificial physics approach to multiple UAVs/ugvs heterogeneous coordination. *Science China Technological Sciences*, 56(10):2473–2479.

Maki, L. R., Galyan, E. L., Chang-Chien, M.-M., and Caldwell, D. R. (1974). Ice nucleation induced by pseudomonas syringae. *Applied microbiology*, 28(3):456–459.

Manabe, S., Stouffer, R., Spelman, M., and Bryan, K. (1991). Transient responses of a coupled ocean–atmosphere model to gradual changes of atmospheric CO2. part i. annual mean response. *Journal of Climate*, 4(8):785–818.

Mason, W. T. (1999). *Fluorescent and luminescent probes for biological activity: a practical guide to technology for quantitative real-time analysis*. Academic Press.

Masutani, S. M. and Adams, E. E. (2001). Experimental study of multi-phase plumes with application to deep ocean oil spills. *Final Report*.

Millner, P. D. (2009). Bioaerosols associated with animal production operations. *Bioresource Technology*, 100(22):5379–5385.

Mishchuk, N. and Goncharuk, V. (2011). Generation and dynamics of aerosols over water surface. *Journal of Water Chemistry and Technology*, 33(2):73–85.

Morris, C., Georgakopoulos, D., and Sands, D. (2004). Ice nucleation active bacteria and their potential role in precipitation. In *Journal de Physique IV (Proceedings)*, volume 121, pages 87–103. EDP sciences.

Morris, C. E., Conen, F., Alex Huffman, J., Phillips, V., Pöschl, U., and Sands, D. C. (2014). Bioprecipitation: a feedback cycle linking earth history, ecosystem dynamics and land use through biological ice nucleators in the atmosphere. *Global change biology*, 20(2):341–351.

Morris, C. E., Monteil, C. L., and Berge, O. (2013). The life history of pseudomonas syringae: linking agriculture to earth system processes. *Annual review of phytopathology*, 51:85–104.

Morris, C. E., Sands, D. C., Vinatzer, B. A., Glaux, C., Guilbaud, C., Buffiere, A., Yan, S., Dominguez, H., and Thompson, B. M. (2008). The life history of the plant pathogen pseudomonas syringae is linked to the water cycle. *The ISME journal*, 2(3):321–334.

Narayanan, S. and Lilly, G. (1993). On the accuracy of xbt temperature profiles. *Deep Sea Research Part I: Oceanographic Research Papers*, 40(10):2105–2113.

Newton, R. J., Jones, S. E., Eiler, A., McMahon, K. D., and Bertilsson, S. (2011). A guide to the natural history of freshwater lake bacteria. *Microbiology and Molecular Biology Reviews*, 75(1):14–49.

Palacios, F. M., Quesada, E. S. E., Sanahuja, G., Salazar, S., Salazar, O. G., and Carrillo, L. R. G. (2017). Test bed for applications of heterogeneous unmanned vehicles. *International Journal of Advanced Robotic Systems*, 14(1):1729881416687111.

Palframan, M. C., Gruszewski, H. A., Schmale III, D. G., and Woolsey, C. A. (2014). Detection of a surrogate biological agent with a portable surface plasmon resonance sensor onboard an unmanned aircraft system. *Journal of Unmanned Vehicle Systems*, 2(4):103–118.

Parker, S. R., West, R. F., Boyd, E. S., Feyhl-Buska, J., Gammons, C. H., Johnston, T. B., Williams, G. P., and Poulson, S. R. (2016). Biogeochemical and microbial seasonal dynamics between water column and sediment processes in a productive mountain lake: Georgetown lake, mt, usa. *Journal of Geophysical Research: Biogeosciences*, 121(8):2064–2081.

Pennington, J., Blum, M., and Chavez, F. (2016). Seawater sampling by an autonomous underwater vehicle:gulper sample validation for nitrate, chlorophyll, phytoplankton, and primary production. *Limnology and Oceanography: Methods*, 14(1):14–23.

Pereira, E., Bencatel, R., Correia, J., Félix, L., Gonçalves, G., Morgado, J., and Sousa, J. (2009). Unmanned air vehicles for coastal and environmental research. *Journal of Coastal Research*, pages 1557–1561.

Pietsch, R. B., Vinatzer, B. A., and Schmale III, D. G. (2017). Diversity and abundance of ice nucleating strains of pseudomonas syringae in a freshwater lake in virginia, usa. *Frontiers in Microbiology*, 8.

Polen, M., Lawlis, E., and Sullivan, R. C. (2016). The unstable ice nucleation properties of snomax® bacterial particles. *Journal of Geophysical Research: Atmospheres*, 121(19).

Polymenakou, P. N. (2012). Atmosphere: a source of pathogenic or beneficial microbes? *Atmosphere*, 3(1):87–102.

Pöschl, U., Martin, S., Sinha, B., Chen, Q., Gunthe, S., Huffman, J., Borrmann, S., Farmer, D., Garland, R., Helas, G., et al. (2010). Rainforest aerosols as biogenic nuclei of clouds and precipitation in the amazon. *science*, 329(5998):1513–1516.

Qian, X., Xiao, Y., Xu, Y., Guo, X., Qian, J., and Zhu, W. (2010). "alive" dyes as fluorescent sensors: fluorophore, mechanism, receptor and images in living cells. *Chemical Communications*, 46(35):6418–6436.

Rashidi, M., Hetsroni, G., and Banerjee, S. (1991). Mechanisms of heat and mass transport at gas-liquid interfaces. *International journal of heat and mass transfer*, 34(7):1799–1810.

Read, T., Bour, O., Bense, V., Le Borgne, T., Goderniaux, P., Klepikova, M., Hochreutener, R., Lavenant, N., and Boschero, V. (2013). Characterizing groundwater flow and heat transport in fractured rock using fiber-optic distributed temperature sensing. *Geophysical Research Letters*, 40(10):2055–2059.

Roberts, G. N. and Sutton, R. (2006). *Advances in unmanned marine vehicles*, volume 69. Iet.

Sabine, C. L., Feely, R. A., Gruber, N., Key, R. M., Lee, K., Bullister, J. L., Wanninkhof, R., Wong, C., Wallace, D. W., Tilbrook, B., et al. (2004). The oceanic sink for anthropogenic CO2. *science*, 305(5682):367–371.

Samset, B. H. (2016). Aerosols and climate.

Sarda, E. I., Qu, H., Bertaska, I. R., and von Ellenrieder, K. D. (2016). Station-keeping control of an unmanned surface vehicle exposed to current and wind disturbances. *Ocean Engineering*, 127:305–324.

Schmale, D., Dingus, B. R., and Reinholtz, C. (2008). Development and application of an autonomous unmanned aerial vehicle for precise aerobiological sampling above agricultural fields. *Journal of Field Robotics*, 25(3):133–147.

Schmale, D., Ross, S., Fetters, T., Tallapragada, P., Wood-Jones, A., and Dingus, B. (2012). Isolates of fusarium graminearum collected 40–320 meters above ground level cause fusarium head blight in wheat and produce trichothecene mycotoxins. *Aerobiologia*, 28(1):1–11.

Schmale III, D. G. and Ross, S. D. (2015). Highways in the sky: Scales of atmospheric transport of plant pathogens. *Annual review of phytopathology*, 53:591–611.

Schumann, T. (1990). On the use of a modified clean-room optical particle counter for atmosperic aerosols at high relative humidity. *Atmospheric Research*, 25(6):499–520.

Schwede, D. B. and Lear, G. G. (2014). A novel hybrid approach for estimating total deposition in the United States. *Atmospheric Environment*, 92:207–220.

Selker, J. S., Thevenaz, L., Huwald, H., Mallet, A., Luxemburg, W., Van De Giesen, N., Stejskal, M., Zeman, J., Westhoff, M., and Parlange, M. B. (2006). Distributed fiber-optic temperature sensing for hydrologic systems. *Water Resources Research*, 42(12).

Shafi, S., Kamili, A. N., Shah, M. A., and Bandh, S. A. (2015). Isolation, identification and distribution of culturable bacteria in manasbal lake, kashmir himalaya. *Proceedings of the National Academy of Sciences, India Section B: Biological Sciences*, pages 1–6.

Shah, B. C., Švec, P., Bertaska, I. R., Sinisterra, A. J., Klinger, W., von Ellenrieder, K., Dhanak, M., and Gupta, S. K. (2016). Resolution-adaptive risk-aware trajectory planning for surface vehicles operating in congested civilian traffic. *Autonomous Robots*, 40(7):1139–1163.

Silva, H., Conceição, R., Wright, M., Matthews, J., Pereira, S., and Shallcross, D. (2015). Aerosol hygroscopic growth and the dependence of atmospheric electric field measurements with relative humidity. *Journal of Aerosol Science*, 85:42–51.

Simmons, D. J. (2004). Corps outlines 6-year plan for claytor lake. *The Roanoke Times [VA]*.

Song, L., Chen, W., Peng, L., Wan, N., Gan, N., and Zhang, X. (2007). Distribution and bioaccumulation of microcystins in water columns: a systematic investigation into the environmental fate and the risks associated with microcystins in meiliang bay, lake taihu. *Water Research*, 41(13):2853–2864.

Stangl, M. J. (2001). An electrofishing raft for sampling intermediate-size waters with restricted boat access. *North American Journal of Fisheries Management*, 21(3):679–682.

Steimle, E. T. and Hall, M. L. (2006). Unmanned surface vehicles as environmental monitoring and assessment tools. In *OCEANS 2006*, pages 1–5. IEEE.

Stiopkin, I. V., Weeraman, C., Pieniazek, P. A., Shalhout, F. Y., Skinner, J. L., and Benderskii, A. V. (2011). Hydrogen bonding at the water surface revealed by isotopic dilution spectroscopy. *Nature*, 474(7350):192–195.

Stokey, R. P., Roup, A., von Alt, C., Allen, B., Forrester, N., Austin, T., Goldsborough, R., Purcell, M., Jaffre, F., Packard, G., et al. (2005). Development of the remus 600 autonomous underwater vehicle. In *OCEANS, 2005. Proceedings of MTS/IEEE*, pages 1301–1304. IEEE.

Suárez, F., Aravena, J., Hausner, M., Childress, A., and Tyler, S. (2011). Assessment of a vertical high-resolution distributed-temperature-sensing system in a shallow thermohaline environment. *Hydrology and Earth System Sciences*, 15(3):1081.

Szwaykowska, K., Romero, L. M.-y.-T., and Schwartz, I. B. (2015). Collective motions of heterogeneous swarms. *IEEE Transactions on Automation Science and Engineering*, 12(3):810–818.

Takahata, K., Shimizu, E., Umeda, A., Oode, T., Tsuchiya, T., and Tamura, Y. (2016). Development of remotely operated unmanned boat with long-range wi-fi. *Artificial Life and Robotics*, 21(3):365–370.

Tang, D., Kester, D. R., Ni, I.-H., Qi, Y., and Kawamura, H. (2003). In situ and satellite observations of a harmful algal bloom and water condition at the pearl river estuary in late autumn 1998. *Harmful Algae*, 2(2):89–99.

Tauro, F., Mocio, G., Rapiti, E., Grimaldi, S., and Porfiri, M. (2012). Assessment of fluorescent particles for surface flow analysis. *Sensors*, 12(11):15827–15840.

Tauro, F., Porfiri, M., and Grimaldi, S. (2016). Surface flow measurements from drones. *Journal of Hydrology*, 540:240–245.

Techy, L., Schmale, D. G., and Woolsey, C. A. (2010). Coordinated aerobiological sampling of a plant pathogen in the lower atmosphere using two autonomous unmanned aerial vehicles. *Journal of Field Robotics*, 27(3):335–343.

Tian, Y., Kang, X., Li, Y., Li, W., Zhang, A., Yu, J., and Li, Y. (2013). Identifying rhodamine dye plume sources in near-shore oceanic environments by integration of chemical and visual sensors. *Sensors*, 13(3):3776–3798.

Touloukian, Y., Powell, R., Ho, C., and Klemens, P. (1970). Thermophysical properties of matter-the tprc data series. volume 1. thermal conductivity-metallic elements and alloys. Technical report, THERMOPHYSICAL AND ELECTRONIC PROPERTIES INFORMATION ANALYSIS CENTER LAFAYETTE IN.

Touloukian, Y. S., Powell, R., Ho, C., and Klemens, P. (1971). Thermophysical properties of matter-the tprc data series. volume 2. thermal conductivity-nonmetallic solids. Technical report, THERMOPHYSICAL AND ELECTRONIC PROPERTIES INFORMATION ANALYSIS CENTER LAFAYETTE IN.

Trenberth, K. E., Fasullo, J. T., and Kiehl, J. (2009). Earth's global energy budget. *Bulletin of the American Meteorological Society*, 90(3):311–323.

Tyler, S. W., Selker, J. S., Hausner, M. B., Hatch, C. E., Torgersen, T., Thodal, C. E., and Schladow, S. G. (2009). Environmental temperature sensing using raman spectra dts fiber-optic methods. *Water Resources Research*, 45(4).

Ukil, A., Braendle, H., and Krippner, P. (2012). Distributed temperature sensing: Review of technology and applications. *IEEE Sensors Journal*, 12(5):885–892.

Valdivieso, M., Haines, K., Balmaseda, M., Chang, Y.-S., Drevillon, M., Ferry, N., Fujii, Y., Köhl, A., Storto, A., Toyoda, T., et al. (2017). An assessment of air–sea heat fluxes from ocean and coupled reanalyses. *Climate Dynamics*, 49(3):983–1008.

Van Emmerik, T., Rimmer, A., Lechinsky, Y., Wenker, K., Nussboim, S., and Van de Giesen, N. (2013). Measuring heat balance residual at lake surface using distributed temperature sensing. *Limnology and Oceanography: Methods*, 11(2):79–90.

Vardy, A. (2016). Aggregation in robot swarms using odometry. *Artificial Life and Robotics*, 21(4):443–450.

Vasilijevic, A., Calado, P., Lopez-Castejon, F., Hayes, D., Stilinovic, N., Nad, D., Mandic, F., Dias, P., Gomes, J., Molina, J., et al. (2015). Heterogeneous robotic system for underwater oil spill survey. In *OCEANS 2015-Genova*, pages 1–7. IEEE.

Vercauteren, N., Huwald, H., Bou-Zeid, E., Selker, J. S., Lemmin, U., Parlange, M. B., and Lunati, I. (2011). Evolution of superficial lake water temperature profile under diurnal radiative forcing. *Water resources research*, 47(9).

Vincent, J. H. (2007). *Aerosol sampling: science, standards, instrumentation and applications*. John Wiley & Sons.

Viswambharan, N., Sathyendranath, S., and Rao, L. G. (1986). Remote sensing of sea surface temperature through infrared radiometry—a review. *Sadhana*, 9(4):281–297.

Vogt, M., Johansson, C., Mårtensson, M., Struthers, H., Ahlm, L., and Nilsson, D. (2013). Heated submicron particle fluxes using an optical particle counter in urban environment. *Atmospheric Chemistry and Physics*, 13(6):3087–3096.

Warren, M., Corke, P., and Upcroft, B. (2016). Long-range stereo visual odometry for extended altitude flight of unmanned aerial vehicles. *The International Journal of Robotics Research*, 35(4):381–403.

Weerasundara, L., Amarasekara, R., Magana-Arachchi, D., Ziyath, A. M., Karunaratne, D., Goonetilleke, A., and Vithanage, M. (2017). Microorganisms and heavy metals associated with atmospheric deposition in a congested urban environment of a developing country: Sri Lanka. *Science of the Total Environment*, 584:803–812.

Weilin, H., Carder, K. L., Costello, D. K., Keping, D., and Zhishen, L. (2003). Using unmanned underwater vehicles as research platforms in coastal ocean studies. *Journal of Ocean University of China (English Edition)*, 2(2):211–217.

Wilhelm, S. W., LeCleir, G. R., Bullerjahn, G. S., McKay, R. M., Saxton, M. A., Twiss, M. R., and Bourbonniere, R. A. (2014). Seasonal changes in microbial community structure and activity imply winter production is linked to summer hypoxia in a large lake. *FEMS microbiology ecology*, 87(2):475–485.

Willis, J. K., Roemmich, D., and Cornuelle, B. (2004). Interannual variability in upper ocean heat content, temperature, and thermosteric expansion on global scales. *Journal of Geophysical Research: Oceans*, 109(C12).

Winter, B. and Chỳlek, P. (1997). Contribution of sea salt aerosol to thè planetary clear-sky albedo. *Tellus B: Chemical and Physical Meteorology*, 49(1):72–79.

Wu, J. (1981). Evidence of sea spray produced by bursting bubbles. *Science*, pages 324–326.

Xu, Z., Khoo, B., and Carpenter, K. (2006). Mass transfer across the turbulent gas–water interface. *AIChE journal*, 52(10):3363–3374.

Yu, Z., Yang, J., Amalfitano, S., Yu, X., and Liu, L. (2014). Effects of water stratification and mixing on microbial community structure in a subtropical deep reservoir. *Scientific reports*, 4.

Yuh, J., Marani, G., and Blidberg, D. R. (2011). Applications of marine robotic vehicles. *Intelligent service robotics*, 4(4):221–231.

Zeeman, M. J., Selker, J. S., and Thomas, C. K. (2015). Near-surface motion in the nocturnal, stable boundary layer observed with fibre-optic distributed temperature sensing. *Boundary-Layer Meteorology*, 154(2):189–205.

Zou, Y., Shi, L., Zhang, S., Liang, C., and Zeng, T. (2016). Oil spill detection by a support vector machine based on polarization decomposition characteristics. *Acta Oceanologica Sinica*, 35(9):86–90.